

AO-A080 245

AIR FORCE INST OF TECH WRIGHT-PATTERSON AFB OH SCH00--ETC F/6 20/6
THE USE OF COMPLEX FIELD VECTORS IN DIFFRACTION THEORY.(U)
DEC 79 M E ROGERS
AFIT/GEP/PH-79D-10

UNCLASSIFIED

NL

1 of 1
ADA
DIR/204

END
DATE
FILMED
11-80
DTIC

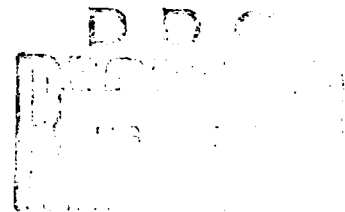
AFIT/GEP/PH/79D-10

THE USE OF COMPLEX FIELD VECTORS
IN DIFFRACTION THEORY

THESIS

AFIT/GEP/PH/79D-10

Mark E. Rogers
1st Lt USAF



Approved for Public Release; Distribution Unlimited.

14

AFIT/GEP/PH/79D-18

9

THE USE OF COMPLEX FIELD VECTORS
IN DIFFRACTION THEORY.

9

Master's THESIS

Presented to the Faculty of the School of Engineering
of the Air Force Institute of Technology
Air University
in Partial Fulfillment of the
Requirements for the Degree of
Master of Science

by
Mark Edward Rogers, B. S.
1st Lt USAF

Graduate Engineering Physics

December 1979

57

312-25

LB

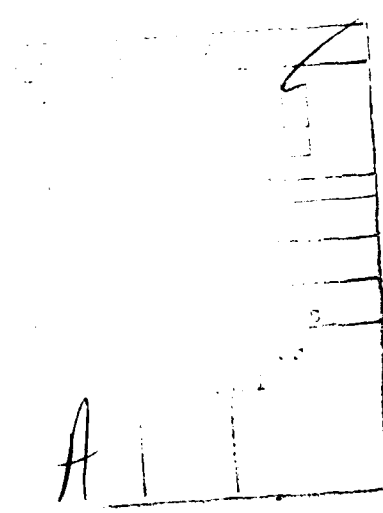
Preface

This work began as an investigation into the various techniques of propagation of EM fields in optical devices. The two simple techniques, geometric optics and scalar diffraction theory, are both based on assumptions that violate Maxwell's equations, except for special cases. The current vector diffraction theories were rigorous, but difficult to apply to various problems. Major Glenn Doughty, who acted as my advisor, had the initial insight of using complex field vectors in the rigorous diffraction problem, which led directly to the development detailed in the first two sections of Chapter III. This insight was so fruitful that we decided to redirect the effort toward developing the complex field vector approach to diffraction theory. The significance of the approach lies in (1) specifying the resultant field in terms of separated component equations, and (2) deriving the Rayleigh-Sommerfeld equation. The second point helps explain where scalar diffraction theory can be an accurate description of a vector field.

I am most indebted to Major Doughty for his insight, guidance and patience in our many hours of discussion. My thanks is also extended to Ms. Sharon Gabriel for her typing assistance. I cannot add sufficient appreciation for my loving wife, Jan, who supported me equally in times of victory and discouragement. Most of all, I thank my Lord Jesus Christ

for His strength and love. As the Great Physicist, He has shown me "great and mighty things" which I did not know. (Jer 33:3) I offer this work to His praise and glory.

Mark E. Rogers



Contents

	Page
Preface.....	ii
List of Figures.....	v
List of Symbols.....	vi
Abstract.....	x
I. Introduction.....	1
II. Theoretical Preliminaries and Past Work.....	5
III. Theoretical Development of the Complex Field Vector Approach in Diffraction.....	13
The Uncoupled Field Equations.....	13
Application to Plane Surfaces.....	16
Discussion of Component Integral Equations..	20
Derivation of Rayleigh-Sommerfeld Equation..	25
IV. Application of the Complex Field Vector Approach.....	28
Preliminary Comments.....	28
Example 1: Linear Polarization.....	30
Example 2: Azimuthal Polarization.....	39
Example 3: Circular Polarization.....	41
Observations on Applications.....	45
V. Conclusions and Recommendations.....	48
Bibliography.....	53
Appendix A: Components of the Vector Integral Equation for \bar{Q}	55
Appendix B: Derivatives of the Green's Function.....	58
Appendix C: Expression of Complex Component Q_+ Using Impedance.....	60
Appendix D: Development of Example 1.....	62
Appendix E: Development of Example 2.....	67
Appendix F: Development of Example 3.....	71
Vita.....	75

List of Figures

<u>Figure</u>		<u>Page</u>
1	Geometry for the General Diffraction Problem..	6
2	Plot of Various Obliquity Factors Where $A = 1 + \cos\theta$, $B = A - \frac{\sin^2\theta}{2}$ and $C = 2\cos\theta$	26
3	Normalized Irradiance Pattern for Initial \bar{E}_1 with $a = 1.2 \mu\text{m}$, $\lambda = 0.6 \mu\text{m}$, and $z = 1 \text{ m}$	31
4	Normalized Irradiance Pattern for Resultant \bar{E}_1 Using the Fast Fourier Transform.....	37
5	Normalized Irradiance Pattern for Resultant \bar{E}_1 Using the Analytic Solution.....	38
6	Normalized Irradiance Pattern for Initial \bar{E}_2 with $a = 6 \mu\text{m}$, $\lambda = 0.6 \mu\text{m}$, and $z = 1 \text{ m}$	40
7	Normalized Irradiance Pattern for Initial \bar{E}_2 ..	42
8	Normalized Irradiance Pattern for Initial \bar{E}_3 with $a = 6 \mu\text{m}$, $\lambda = 0.6 \mu\text{m}$, and $z = 1 \text{ m}$	43
9	Normalized Irradiance Pattern for Resultant \bar{E}_3	46

List of Symbols

$J_1(x)$	Bessel function of first kind of order one for x
k	Wave number, $k = \frac{2\pi}{\lambda} = \omega\sqrt{\mu\epsilon}$
k_z	Component of \bar{k} in \hat{a}_z direction
k_ρ	Component of \bar{k} in \hat{a}_ρ direction
L	Length of the data window
N	Number of samples taken in data window
\hat{n}	Unit normal to some surface
\bar{P}	Complex field vector, $\bar{P} = \mu\bar{H} - i\sqrt{\mu\epsilon} \bar{E}$
$P_x, P_y, P_z, P_\rho, P_\phi$	Components of \bar{P}
P_\pm	Complex component, $P_\pm = P_x \pm iP_y$
\bar{Q}	Complex field vector, $\bar{Q} = \mu\bar{H} + i\sqrt{\mu\epsilon} \bar{E}$
$Q_x, Q_y, Q_z, Q_\rho, Q_\phi$	Components of \bar{Q}
Q_\pm	Complex component, $Q_\pm = Q_x \pm iQ_y$
R	Distance between source point and observation point, $R = \underline{r-r}' $
\bar{r}'	Vector locating the source point
\bar{r}	Vector locating the observation point
$\overline{r-r}'$	Vector difference between \bar{r} and \bar{r}'
S	Open surface on which the resultant field is expressed
S'	Open surface on which the initial field is expressed
S_c	Arbitrary closed surface
S_1	Plane surface such that $S = S_1 + S_2$
S_2	Hemispherical surface centered at observation

List of Symbols

$T(x)$	Aperture function that allows limits on a finite integral to be expanded to $(-\infty, \infty)$
u	Scalar wave function
v	Complex scalar, $v = 1/\sqrt{\mu\epsilon}$; magnitude of v is speed of propagation in medium
(x, y, z)	Ordered triple for rectangular coordinates
<u>Greek</u>	
α, β	Angles defined by $\sin\alpha = \frac{x-x'}{R}$ and $\sin\beta = \frac{y-y'}{R}$
δ	Angle defined by $\tan\delta = \frac{x-x'}{y-y'}$
δ_{ij}	Kronecker delta
ϵ	Dielectric constant for medium
$\tilde{\epsilon}$	Complex dielectric constant for conducting medium; here $\tilde{\epsilon} = \epsilon - i\frac{\sigma}{\omega}$
$\tilde{\epsilon}_1$	Complex dielectric constant used by Doughty (Ref 7)
n	Intrinsic impedance of medium
$n_{xy}^{\pm}, n_{yx}^{\pm}$	Wave impedances for EM field
θ	Angle defined by $\theta = \cos^{-1}\left(\frac{\hat{n}\cdot\overline{r-r'}}{R}\right)$
λ	Wavelength
μ	Magnetic permeability of medium
π	Constant where $\pi = 4\tan^{-1}(1) = 3.141592654$
ρ	Radius of circle; radial component in cylindrical coordinates

List of Symbols

(ρ, ϕ, z)	Ordered triple for cylindrical coordinates
σ	Conductivity of medium
ϕ	Scalar part of dyadic Green's function, $\phi = \frac{e^{-ikR}}{4\pi R}$
$\phi_{,x}$	Abbreviation for $\frac{\partial}{\partial x}(\phi)$
$\phi_{,yx}$	Abbreviation for $\frac{\partial^2}{\partial x \partial y}(\phi)$
ϕ_1	Scalar Green's function, $\phi_1 = \frac{e^{ikR}}{R}$
ϕ	Angular component in polar coordinate
ω	Angular frequency

Abstract

A rigorous solution to the diffraction problem is obtained by using two complex field vectors: $\bar{Q} = \mu\bar{H} + i\sqrt{\mu\epsilon}\bar{E}$ and $\bar{P} = \mu\bar{V} - i\sqrt{\mu\epsilon}\bar{E}$. The derivation begins with Maxwell's equations that are uncoupled in terms of \bar{Q} and \bar{P} . Then, following the work of Stratton and Chu and that of Doughty, the field equations are integrated directly to yield a pair of uncoupled vector integral equations involving the tangential components of \bar{Q} and \bar{P} on some open surface S' . When S' is planar, the equations are expanded in a more useable set of six component integral equations. The main assumptions in the derivation of these latter equations are that the initial \bar{E} and \bar{H} must satisfy Maxwell's equation on S' and that the resultant field must be calculated for $k \gg 1/R$. For the case where (1) the initial field is traveling normal to S' , and (2) the resultant field is calculated only in the region near the optical axis, the expressions for the tangential components of the resultant \bar{E} are identical in form with the Rayleigh-Sommerfeld equation of scalar diffraction theory. Three examples are developed to show the method of applying complex field vectors to diffraction problems and to show the agreement on axis with the results calculated from the Rayleigh-Sommerfeld equation. The examples also provide insight into the diffraction process by discussing the approximations made in obtaining the resultant field near the axis. Thus, the complex field vector approach provides a rigorous, yet simple and straightforward, method of solving the diffraction problem.

THE USE OF COMPLEX FIELD VECTORS
IN DIFFRACTION THEORY

I. Introduction

The goal of the general diffraction problem is to calculate a resultant electromagnetic field on some surface S from an initial electromagnetic field on some surface S' . Building on the work of Huygens, Fresnel, Kirchoff and others, many authors (e.g., Refs 1-5) have taken various approaches to solving this problem. However, the two basic approaches are both based in principle on Maxwell's equations. The first approach deals rigorously with the vector nature of the EM field, and is known as vector diffraction theory. The second approach assumes that each field component may be considered independently. This scalar diffraction theory is suggested by the separate wave equations for the electric and magnetic field intensities, \vec{E} and \vec{H} , that are obtainable from Maxwell's equations. However, the "real problem is not the integration of a wave equation, either scalar or vector, but of a simultaneous system of first-order vector equations relating the vectors \vec{E} and \vec{H} ." (Ref 6:463) Unfortunately, the inherent coupling of \vec{E} and \vec{H} makes the rigorous solution of the general diffraction problem difficult to obtain.

The vector diffraction theories have some common advantages and disadvantages. Each is a rigorous solution to Maxwell's equations for a given set of assumptions and boundary conditions. However, the resulting expressions are often difficult to apply to general problems and may obscure the underlying physical phenomena involved in diffraction.

Scalar diffraction theory is a more phenomenological approach, but it is more easily applied and quite accurate in certain regions. The approach, which is a rigorous description of the propagation of sound waves, is suggested by the separation of the vector wave equations for \vec{E} and \vec{H} into six scalar wave equations when rectangular coordinates are used. However, the assumption that each component is independent ignores the inherent coupling of \vec{E} and \vec{H} , and the results generally do not satisfy Maxwell's equations.

From the above discussion, we see that no approach is both rigorous and easily applied. The goal of this work is to develop a theory of diffraction that incorporates the advantages of the vector and scalar approaches while avoiding some of the shortcomings. Specifically, the primary objective of this work is to develop an approach to diffraction that uses complex field vectors to recast Maxwell's equations into a set of separated integral equations that describe the resultant EM field. Two secondary objectives are: (1) to show that scalar diffraction theory is a special case of this approach, and (2) to show that this approach is readily

applicable to various diffraction problems. A minor objective in this application is to gain some familiarity with Fast Fourier Transform techniques as applied to the computation of solutions to diffraction problems. The objective of this report is to describe the development and application of this approach to the general diffraction problem.

The use of complex field vectors, $\bar{Q} = \mu\bar{H} + i\sqrt{\mu\epsilon}\bar{E}$ and $\bar{P} = \mu\bar{H} - i\sqrt{\mu\epsilon}\bar{E}$, has two significant features. The first feature is the development of a set of uncoupled vector integral equations that retain the vector nature of the EM field. The component equations that result from this decoupling are easily applied, interpreted and understood, and yet they are still rigorously based on Maxwell's equations. The second contribution is the substantiation of scalar diffraction theory under conditions common to many diffraction problems.

This presentation begins with a review of past work and a discussion of some theoretical preliminaries, both of which are contained in Section II. This review is intended to set the stage for later developments, and is not an exhaustive history of diffraction theory. The theoretical preliminaries provide the background for the theoretical development of the complex field vector approach in Section III. Three example fields are examined in Section IV to

illustrate the application of this approach. Section V contains the conclusions and recommendations. Various appendices contain detailed mathematical developments to support this work. All equations will be in MKS units unless otherwise specified.

II. Theoretical Preliminaries and Past Work

This section develops the geometry for the general diffraction problem, discusses the type of medium assumed in this report, and derives some preliminary relations based on Maxwell's equations. The section also includes a discussion of two areas of past work that are relevant to this report. The first is a direct integration of Maxwell's equations as developed by Stratton and Chu (Ref 4) and extended by Doughty (Ref 7); the second is the Rayleigh-Sommerfeld formulation of scalar diffraction theory.

The reader interested in a more in-depth treatment of vector diffraction theory is referred to the paper by Kottler (Ref 2), the article by Bouwkamp (Ref 5), the treatment by Born and Wolf (Ref 8:556), or the book by Baker and Copson (Ref 9:102). Scalar diffraction theory is discussed in most texts on physical optics, such as the text by Born and Wolf (Ref 8:320). The Rayleigh-Sommerfeld formulation described in this section is based on the discussion in Goodman (Ref 10:30).

Theoretical Preliminaries

Figure 1 shows the geometry for the general diffraction problem used in this report. The initial EM field is assumed to be non-zero only on the open surface S' ; values on S' will be denoted using primes. The resultant

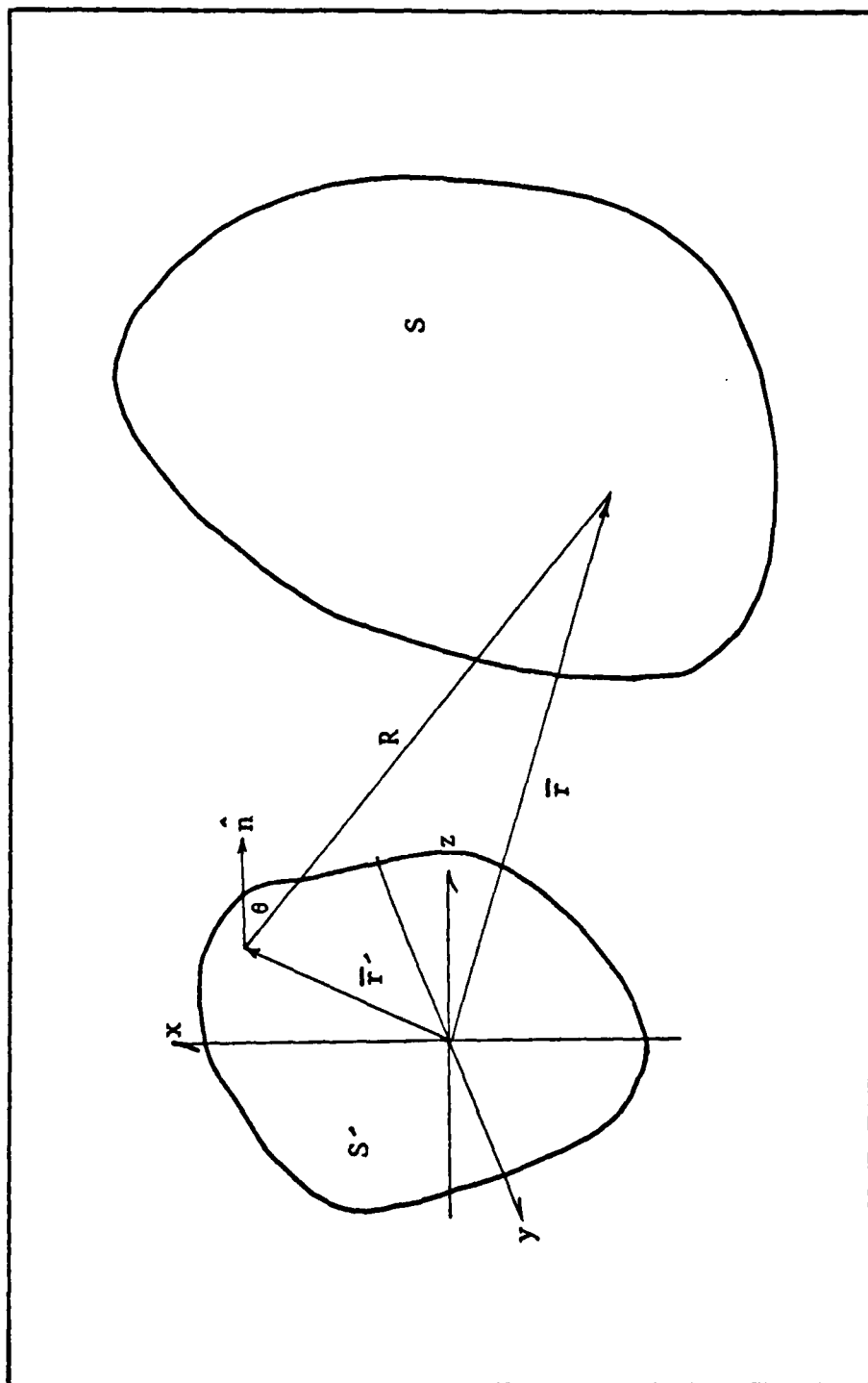


Figure 1. Geometry for the General Diffraction Problem

EM field is described on some open surface S ; values on S will be unprimed. The distance from a source point on S' to an observation point on S is given by $R = |\overline{r-r'}$ and the angle θ is defined by the angle between $\overline{r-r'}$ and \hat{n} , where \hat{n} is a unit normal to S' pointing toward the surface S . The origin is chosen to lie on the S' such that if S' and S were plane surfaces, the points on S' would be described by $(x',y',0)$ and those on S by (x,y,z) . For many applications, S' and S will be planes, but in the general equations they need not be so restricted.

Throughout this report, the propagation medium will be assumed to be homogeneous, isotropic, linear and free of charge, unless otherwise stated. Ohm's Law is assumed to hold in the medium, unless otherwise stated. Under these assumptions, Maxwell's equations can be written as follows:

$$\nabla \times \overline{E}(\overline{r},t) = -\mu \frac{\partial}{\partial t} [\overline{H}(\overline{r},t)] \quad (1)$$

$$\nabla \times \overline{H}(\overline{r},t) = \epsilon \frac{\partial}{\partial t} [\overline{E}(\overline{r},t)] + \sigma \overline{E} \quad (2)$$

$$\nabla \cdot \overline{E}(\overline{r},t) = 0 \quad (3)$$

$$\mu \nabla \cdot \overline{H}(\overline{r},t) = 0 \quad (4)$$

Both \vec{E} and \vec{H} can be expanded here in normal modes, as shown in Eq (5) for an arbitrary vector \vec{A} .

$$\vec{A}(\vec{r}, t) = \frac{1}{(2\pi)^3} \int_{-\infty}^{\infty} \vec{A}(\vec{r}, \omega) e^{i\omega t} d\omega \quad (5)$$

Using these expansions in Eqs (1) and (2), one finds for an arbitrary frequency ω ,

$$\nabla \times \vec{E}(\vec{r}) + i\omega\mu \vec{H}(\vec{r}) = 0 \quad (6)$$

$$\nabla \times \vec{H}(\vec{r}) - i\omega\epsilon \vec{E}(\vec{r}) = 0 \quad (7)$$

where the frequency dependence has been suppressed and the complex dielectric constant is defined as $\tilde{\epsilon} = \epsilon - i \frac{\sigma}{\omega}$. Equations (6) and (7) provide the starting point for the development in Section III. Before this development begins, however, it will be useful to review some past work that is relevant to this report.

Past Work

A Vector Diffraction Theory. Stratton and Chu developed an analytic solution to the diffraction problem by direct integration of Maxwell's equations using a vector analogue to Green's theorem (Ref 4 or Ref 6:464). For a nonconducting medium, they obtained the resultant \vec{E} and \vec{H} at any point on the interior of a volume V bounded by a closed surface S_c , where

\bar{E} and \bar{H} are expressed as the sum of a volume integral and an integral over S_c . The initial field is specified on S_c . By assuming the volume to be free of charge and current and the initial field to be non-zero only on some finite portion of S_c , say S' , the integral equations for \bar{E} and \bar{H} can be rewritten as the sum of an integral over S' and an integral on the contour c' enclosing S' . These equations, Eqs (8) and (9), are equivalent to those derived by Kottler (Ref 2).

$$\begin{aligned} \bar{E}(\bar{r}) &= \frac{1}{i\omega\epsilon} \frac{1}{4\pi} \oint_{c'} \nabla\phi_1 \bar{H}' \cdot d\bar{S} \\ &- \frac{1}{4\pi} \int_{S'} [i\omega\mu(\hat{n}\times\bar{H}')\phi_1 + (\hat{n}\times\bar{E}')\times\nabla\phi_1 + (\hat{n}\cdot\bar{E}')\nabla\phi_1] dS' \end{aligned} \quad (8)$$

$$\begin{aligned} \bar{H}(\bar{r}) &= \frac{1}{i\omega\mu} \frac{1}{4\pi} \oint_{c'} \nabla\phi_1 \bar{E}' \cdot d\bar{S} \\ &+ \frac{1}{4\pi} \int_{S'} [i\omega\epsilon(\hat{r}\times\bar{E}')\phi_1 - (\hat{n}\times\bar{H}')\times\nabla\phi_1 - (\hat{n}\cdot\bar{H}')\nabla\phi_1] dS' \end{aligned} \quad (9)$$

where $\phi_1 = \exp [ikR]/R$. In a parallel development, Doughty (Ref 7:21) developed an analogous set of equations for the case where Ohm's Law holds in the medium and without

assuming the initial field is zero everywhere except on S' . For the diffraction problem, Doughty's approach is equivalent to that of Stratton and Chu. Taking the curl of Doughty's equations, one obtains

$$\bar{E}(\bar{r}) = \int_{S'} \left[-\frac{i}{\omega \epsilon_1} (\hat{n} \times \bar{H}') \cdot \nabla \times \nabla \times \bar{G} + \nabla \times \bar{G} \cdot (\hat{n} \times \bar{E}') \right] dS' \quad (10)$$

$$\bar{H}(\bar{r}) = \int_{S'} \left[\frac{i}{\omega \mu} (\hat{n} \times \bar{E}') \cdot \nabla \times \nabla \times \bar{G} + \nabla \times \bar{G} \cdot (\hat{n} \times \bar{H}') \right] dS' \quad (11)$$

where ϵ_1 is a complex dielectric constant that accounts for the absorption or gain in a medium, and ∇' refers to the gradient with respect to the primed coordinates (x', y', z') , and \bar{G} is the dyadic Green's function,

$$\bar{G} = \bar{I} \phi = (\hat{a}_x \hat{a}_x + \hat{a}_y \hat{a}_y + \hat{a}_z \hat{a}_z) \phi \quad (12)$$

where

$$\phi = \exp[-ikR]/4\pi R \quad (13)$$

where $R = |\bar{r} - \bar{r}'|$. The resultant EM field expressed by Eqs (10) and (11) is a solution to Maxwell's equations but, owing to the coupling of \bar{E} and \bar{H} , the system of equations is not readily solved.

Rayleigh-Sommerfeld Formulation. A brief discussion of scalar diffraction theory highlights its phenomenological nature, and provides background for Sections III and IV. The underlying assumption is that light can be treated as a scalar phenomenon, described by some scalar wave function $u(\vec{r})$ that satisfies the scalar Helmholtz equation,

$$(\nabla^2 + k^2) u(\vec{r}) = 0 \quad (14)$$

where the wave number $k = \omega\sqrt{\mu\epsilon} = \frac{2\pi}{\lambda}$. $u(\vec{r})$ is phenomenologically interpreted as one of the transverse components of \vec{E} or \vec{H} . By using Green's theorem, the value of $u(\vec{r})$ within a volume V can be represented as an integral over a closed surface S_c that depends on the values of u on S_c and a scalar Green's function G that satisfies Eq (14). The closed surface can be partitioned into a plane surface S_1 and a hemispherical surface S_2 . The integral on S_2 approaches zero as the surface is expanded toward infinity, provided $u(\vec{r})$ meets the Sommerfeld radiation condition. Then the resultant function is represented by

$$u(\vec{r}) = \frac{1}{4\pi} \int_{S_1} \frac{\partial u(\vec{r}')}{\partial n} G(\vec{r}-\vec{r}') - \frac{\partial G(\vec{r}-\vec{r}')}{\partial n} u(\vec{r}') dS_1 \quad (15)$$

where $\frac{\partial}{\partial n}$ denotes the derivative with respect to \hat{n} . The infinite plane S_1 is usually broken into two regions, an aperture (such as the open surface S') and the region

exterior to the aperture. Choosing G to be ϕ as defined by Eq (13) leads to specifying both u and $\frac{\partial u}{\partial n}$ to be zero except on S' , which are inconsistent boundary conditions. Sommerfeld showed that a Green's function exists that is zero on the plane surface S_1 and thus the boundary conditions are reduced to specifying $u(\vec{r}')$ to be zero except on S' . Then Eq (15) becomes

$$u(\vec{r}) = \frac{i}{\lambda} \int_{S'} u(\vec{r}') \frac{e^{-ikR}}{R} \cos \theta \, dS' \quad (16)$$

where θ was defined in the preceding section. Using Eq (13), the above equation can be rewritten:

$$u(\vec{r}) = ik \int_{S'} u(\vec{r}') (2 \cos \theta) \phi \, dS' \quad (17)$$

Both Eqs (16) and (17) are forms of the Rayleigh-Sommerfeld equation, which is mathematically consistent, but was obtained by assuming each field component is independent. In spite of this deficiency, the irradiance patterns do agree with experimental results when θ is small (Refs 11, 12).

Equations (10), (11), and (17) are important results that will be used in the development and application of the complex field vector approach. This development is the subject of the next section.

III. Theoretical Development of the Complex Field Vector Approach in Diffraction

The purpose of this chapter is to solve the diffraction problem with complex field vectors. In the first section below, these vectors are introduced and the resultant electromagnetic field is expressed by a set of uncoupled vector integral equations over open surfaces. The integral equations are then specialized to open planar surfaces; so then the resultant field is described by six component integral equations. A discussion of these six equations provides insight into the diffraction process. The chapter closes by deriving the Rayleigh-Sommerfeld equation from these component equations.

The Uncoupled Field Equations

As stated earlier, several different approaches could be taken to rigorously solve the diffraction problem. Since most practical problems are based on a knowledge of the initial field, a solution based directly on that knowledge seems most useful. For this reason, the approach taken here follows that of Stratton and Chu (see Section II) and relies on a knowledge of the initial field intensity vectors, \bar{E} and \bar{H} .

Let the complex field vectors be defined as in Eqs (18) and (19).

$$\bar{Q}(\bar{r}) = \mu \bar{H}(\bar{r}) + i \sqrt{\mu \epsilon} \bar{E}(\bar{r}) \quad (18)$$

$$\bar{P}(\bar{r}) = \mu \bar{H}(\bar{r}) - i \sqrt{\mu \epsilon} \bar{E}(\bar{r}) \quad (19)$$

Others have used combinations of \bar{E} and \bar{H} to reduce Maxwell's equations to particularly compact form (Refs 9, 13, 14). The definitions used here follow Stratton (Ref 4:32), but the forms in Eqs (18) and (19) were first suggested for application to the diffraction problem by Doughty (Ref 15). Note that these complex field vectors retain the proper phase relationship in the field. In \bar{P} , \bar{E} is advanced by 90° ; in \bar{Q} , \bar{E} is retarded by 90° . Equations (18) and (19) are solved for \bar{E} and \bar{H} to obtain the equations,

$$\bar{E} = -\frac{iv}{2} (\bar{Q} - \bar{P}) \quad (20)$$

$$\bar{H} = \frac{1}{2\mu} (\bar{Q} + \bar{P}) \quad (21)$$

where $v = 1/\sqrt{\mu \epsilon}$. Substituting these expressions into Eqs (6) and (7), one can solve the equations simultaneously to obtain uncoupled equations in \bar{Q} and \bar{P} :

$$\nabla \times \bar{Q} = k\bar{Q} \quad (22)$$

$$\nabla \times \bar{P} = -k\bar{P} \quad (23)$$

Applying these equations, as well as the definitions of \bar{Q} and \bar{P} , Eqs (10) and (11) can be manipulated by first multiplying Eq (10) by $i\sqrt{\mu\epsilon}$ and Eq (11) by μ , and then adding or subtracting Eq (10) from Eq (11) to yield two uncoupled integral equations over open surfaces that depend on the values of \bar{Q} and \bar{P} on the open surface, as shown in Eqs (24) and (25).

$$\bar{Q}(\bar{r}) = \int_{S'} \{ [\hat{n} \times \bar{Q}'(\bar{r}')] \cdot \nabla \times \bar{G} + \frac{1}{k} [\hat{n} \times \bar{Q}'(\bar{r}')] \cdot \nabla \times \nabla' \times \bar{G} \} dS' \quad (24)$$

$$\bar{P}(\bar{r}) = \int_{S'} \{ [\hat{n} \times \bar{P}'(\bar{r}')] \cdot \nabla \times \bar{G} - \frac{1}{k} [\hat{n} \times \bar{P}'(\bar{r}')] \cdot \nabla \times \nabla' \times \bar{G} \} dS' \quad (25)$$

Recall that \bar{G} is the dyadic Green's function defined in Eq (12). The above equations represent the resultant field due to the initial field on S' , since \bar{E} and \bar{H} can be obtained via Eqs (20) and (21).

To properly use Eqs (24) and (25), the initial field used to form Q' and P' must be a valid EM field on S' . Thus, either \bar{E}' , \bar{H}' or the tangential components of \bar{E}' and \bar{H}' on the surface S' must be known in order

to obtain the resultant field. The same knowledge of the initial field would permit Eqs (10) and (11) to be solved, but Eqs (24) and (25) are simpler to use because they are uncoupled. But even these equations are cumbersome. In the next section, we will use these equations to generate a set of six component integral equations on S' that are not only quite easy to apply, but reveal a good deal about the diffraction process.

Application to Plane Surfaces

Let S' be a plane surface, and choose $\hat{n} = +\hat{a}_z$. Consider first the integrand in Eq (24). By replacing \hat{n} with $+\hat{a}_z$, the cross product of \hat{n} and \bar{Q} decomposes \bar{Q} into transverse components. The continued expansion of the integrand into components is facilitated by recalling $R = |\bar{r} - \bar{r}'|$ which leads to the relationship $\nabla\phi = -\nabla'\phi$. Calculating the derivatives and taking the scalar product of $\bar{Q}(\bar{r})$ with \hat{a}_x , \hat{a}_y and \hat{a}_z sequentially, Eq (24) can be decomposed into three scalar equations: (Appendix A contains details of this decomposition.)

$$Q_x = \int_{S'} \{-Q_x^{\phi},_z - \frac{1}{k}[Q_y^{\phi}(k^2\phi + \phi_{,xx}) - Q_x^{\phi},_{xy}]\} dS' \quad (26)$$

$$Q_y = \int_{S'} \{-Q_y^{\phi},_z - \frac{1}{k}[-Q_x^{\phi}(k^2\phi + \phi_{,xx}) + Q_y^{\phi},_{yx}]\} dS' \quad (27)$$

$$Q_z = \int_{S'} \{Q_x^{\phi},_x + Q_y^{\phi},_y + \frac{1}{k}[Q_x^{\phi},_{zy} - Q_z^{\phi},_{zx}]\} dS' \quad (28)$$

where the notation on the terms containing ϕ represent the derivatives of ϕ with respect to the subscripted variable; for example, $\phi_{,x} = \frac{\partial \phi}{\partial x}$ and $\phi_{,xy} = \frac{\partial^2 \phi}{\partial x \partial y}$. Assuming $k \gg 1/R$, which restricts the evaluation of the resultant EM field to be at least several wavelengths from surface S' , the generalized first and second derivatives are approximated by Eqs (29) and (30), respectively.

(See Appendix B.)

$$\phi_{,x_i} = -ik\phi \frac{x_i - x'_i}{R} \quad (29)$$

$$\phi_{,x_i x_j} = -\frac{ik\phi}{R} \delta_{ij} - k^2 \phi \frac{(x_i - x'_i)(x_j - x'_j)}{R^2} \quad (30)$$

where x_ℓ is associated with the values x , y , and z as ℓ ranges from 1 to 3, respectively. Using these derivatives and the definitions below

$$\sin \alpha \equiv \frac{x - x'}{R} \quad ; \quad \sin \beta \equiv \frac{y - y'}{R} \quad ; \quad \cos \theta \equiv \frac{z - z'}{R}$$

one obtains three integral expressions for the components of \bar{Q} , as indicated in Eqs (31) through (33)

$$Q_x = k \int_{S'} \phi [Q'_x (i \cos \theta - \sin \alpha \sin \beta) - Q'_y (1 - \sin^2 \alpha)] dS' \quad (31)$$

$$Q_y = k \int_{S'} \phi [Q'_y (i \cos \theta + \sin \alpha \sin \beta) + Q'_x (1 - \sin^2 \beta)] dS' \quad (32)$$

$$Q_z = k \int_{S'} \phi [-Q'_x (i \sin \alpha + \sin \beta \cos \theta) - Q'_y (i \sin \beta - \sin \alpha \cos \theta)] dS' \quad (33)$$

These equations are written in a particularly compact form by introducing the complex components defined in Eq (34) with an analogous definition for the components P_{\pm} . These components are an alternate way of decomposing \bar{Q} and \bar{P} into components. Although their transformation properties are more complicated than their rectangular counterparts, these components lend particular insight into the diffraction process, as will be discussed in the next section.

$$Q_{\pm} \equiv Q_x \pm i Q_y \quad (34)$$

Using this definition as well as the definition that $\delta = \tan^{-1} (\sin\alpha/\sin\beta)$ and the angular relationship $\sin^2\theta = \sin^2\alpha + \sin^2\beta$ which is obtained from the definition of R , Eqs (31) through (33) become Eqs (35) through (37).

$$Q_+ = ik \int_{S^-} [Q_+^i (\cos\theta + 1 - \frac{\sin^2\theta}{2}) - \frac{1}{2} Q_-^i \sin^2\theta e^{-2i\delta}]_{\phi} dS^i \quad (35)$$

$$Q_- = ik \int_{S^-} [Q_-^i (\cos\theta - 1 + \frac{\sin^2\theta}{2}) + \frac{1}{2} Q_+^i \sin^2\theta e^{2i\delta}]_{\phi} dS^i \quad (36)$$

$$Q_2 = \frac{k}{2} \int_{S^-} [Q_+^i (1 + \cos\theta) e^{i\delta} - Q_-^i (1 - \cos\theta) e^{-i\delta}]_{\phi} \sin\theta dS^i \quad (37)$$

By a similar series of steps, Eqs (38) through (40) can be obtained for $\bar{P}(\bar{r})$:

$$P_+ = ik \int_{S'} [P'_+(\cos\theta-1 + \frac{\sin^2\theta}{2}) + \frac{1}{2} P'_- \sin^2\theta e^{-2i\delta}] \phi dS' \quad (38)$$

$$P_- = ik \int_{S'} [P'_-(\cos\theta+1 - \frac{\sin^2\theta}{2}) - \frac{1}{2} P'_+ \sin^2\theta e^{2i\delta}] \phi dS' \quad (39)$$

$$P_z = \frac{k}{2} \int_{S'} [P'_+(1-\cos\theta)e^{i\delta} - P'_-(1+\cos\theta) e^{-i\delta}] \phi \sin\theta dS' \quad (40)$$

Equations (35) through (40) are the six component integral equations that are used to find the resultant EM field if S' is a plane. The initial \bar{E} and \bar{H} are assumed to satisfy Maxwell's equations, and the component equations were developed with the approximation $k \gg 1/R$. One should note here that the methodology of using the complex field vectors in diffraction begins by taking \bar{E} and \bar{H} on plane S' and forming \bar{Q}' and \bar{P}' . These vectors retain the coupling of \bar{E} and \bar{H} , but allow the resultant field to be expressed by the six component equations given above. Using the definitions of Q_{\pm} and P_{\pm} , Eqs (20) and (21) can be rewritten in a form that facilitates reforming the resultant field in terms of \bar{E} and \bar{H} . Eqs (41) through (43) show the relationships for \bar{E} .

$$E_x = -\frac{iv}{4} (Q_+ + Q_- - P_+ - P_-) \quad (41)$$

$$E_y = \frac{v}{4} (Q_- - Q_+ - P_- + P_+) \quad (42)$$

$$E_z = -\frac{iv}{2} (Q_z - P_z) \quad (43)$$

The set of scalar integral equations is a mathematically simple yet rigorous solution to the diffraction problem.

Discussion of Component Integral Equations

In this section we analyze three terms that occur in Eqs (35) through (40), namely the complex components Q_{\pm} and P_{\pm} , the term δ , and the angular dependence (which is also called the obliquity factor).

The Complex Components. To investigate the nature of Q_{\pm} and P_{\pm} , we discuss their definition using polar coordinates, their expression in terms of impedances, and their circularly polarized nature.

First, the components can be readily expressed in cylindrical coordinates, as shown in Eq (44):

$$Q_{\pm} = (Q_{\rho} \pm i Q_{\phi}) e^{\pm i\phi} \quad (44)$$

where the transformation matrix in Eq (45) has been used.

$$\begin{pmatrix} x \\ y \\ z \end{pmatrix} = \begin{pmatrix} \cos\phi & -\sin\phi & 0 \\ \sin\phi & \cos\phi & 0 \\ 0 & 0 & 1 \end{pmatrix} \begin{pmatrix} \rho \\ \phi \\ z \end{pmatrix} \quad (45)$$

The expression in Eq (44) and the analogous expression for P_{\pm} are useful in problems with cylindrical symmetry, since the component integral equations can still be used in their present form.

Next, the complex scalar Q_{\pm} is rewritten in terms of intrinsic and wave impedances, using Eqs (18) and (34) as well as the definition of the intrinsic and wave impedances (Ref 16:87):

$$\eta = \sqrt{\frac{\mu}{\epsilon}} \quad (46)$$

$$\frac{E_x}{H_y} = +\eta_{xy+} = -\eta_{xy-} \equiv \pm\eta_{xy\pm} \quad (47)$$

$$\frac{E_y}{H_x} = -\eta_{yx+} = \eta_{yx-} \equiv \mp\eta_{yx\pm} \quad (48)$$

The + sign on the subscripts of the wave impedances refers to positive z propagation, while the - sign refers to negative z propagation. The order of x and y indicates which ratio of components is implied. Finally, the combined symbol using the ambiguous sign allows the equations using the wave impedances to be written in a compact manner. The resulting equations for Q_+ and Q_- are shown in Eqs (49) and (50). (See Appendix C.) An analogous procedure can be applied to P_{\pm} .

$$Q_+ = -\sqrt{\mu\epsilon} E_y \left(1 \pm \frac{n}{n_{yx}}\right) + i \sqrt{\mu\epsilon} E_x \left(1 \pm \frac{n}{n_{xy}}\right) \quad (49)$$

$$Q_- = \sqrt{\mu\epsilon} E_y \left(1 \pm \frac{n}{n_{yx}}\right) + i \sqrt{\mu\epsilon} E_x \left(1 \pm \frac{n}{n_{xy}}\right) \quad (50)$$

Recalling the time factor is $e^{i\omega t}$, and writing $\bar{E} = E_+ \hat{a}_+ + E_- \hat{a}_-$ where

$$\hat{a}_{\pm} = \frac{1}{\sqrt{2}} (\hat{a}_x \pm i \hat{a}_y) \quad (51)$$

one can show that E_+ is associated with right circular polarization and E_- with left circular polarization for +z propagation, and vice versa for -z propagation.

For uniform plane waves, $|\eta_{xy}| = |\eta_{yx}| = |\eta|$. Then, for a uniform plane wave propagating in the $+z$ direction, Eqs (49) and (50) become

$$Q_+ = 2i \sqrt{\mu\epsilon} (E_x + i E_y) = 2\sqrt{2} i \sqrt{\mu\epsilon} E_- \quad (52)$$

$$Q_- = 0 \quad (53)$$

The expressions for P_{\pm} are $P_+ = 0$ and

$$P_- = -2i \sqrt{\mu\epsilon} (E_x - i E_y) = -2\sqrt{2} i \sqrt{\mu\epsilon} E_+ \quad (54)$$

A similar analysis for the $-z$ direction reveals that Q_{\pm} is identified as left circular and P_{\pm} as right circular. For predominantly $+z$ propagation, where $\vec{K} = k \hat{a}_z$, Q_- and P_+ are negligible, while Q_+ and P_- are negligible for $-z$ propagation. Since the quantities Q_{\pm} and P_{\pm} are components, they do contain the vector sense of direction and polarization. Any polarization state can be formed with P_{\pm} and Q_{\pm} by the proper choice of E_+ and E_- .

We have seen that the complex components can be expressed in either rectangular or cylindrical coordinates. The components are dependent on both the medium and the ratio of the field vectors, and they contain the vector nature of the field as shown by the inherent circular polarization and directionality of Q_{\pm} and P_{\pm} for predominantly $\pm z$ propagation.

The δ Term. This term represents a spatial phase shift between the initial field and the resultant field since δ can be expressed as

$$\delta = \tan^{-1} \left(\frac{x - x'}{y - y'} \right) \quad (55)$$

This term is the only one in the integrand that is linear in $(x-x')$ and $(y-y')$. It is also worth noting that each term containing δ is also directly related to the angle θ , so as θ gets small, the sense of orientation is weakened. This explains in part why scalar diffraction theory is accurate in the paraxial region (where θ is small).

Obliquity Factors. A comparison of the various obliquity factors sets the stage for the derivation of the Rayleigh-Sommerfeld equation in the next section. Consider again an initial field traveling in the predominantly $+z$ direction. Then, for angles less than about 45° , Eqs (35) and (39) dominate Eqs (36) and (38) in terms of magnitude, since $Q_+^- \gg Q_-^-$ and $P_-^- \gg P_+^-$ and $\cos\theta > \sin^2\theta$. Notice that the term $(\cos\theta + 1 - \frac{\sin^2\theta}{2})$ is common to both Eqs (35) and (39). This term can be compared against the obliquity factor of the Fresnel-Kirchhoff formulation of scalar diffraction theory, $1 + \cos\theta$, and that of the Rayleigh-Sommerfeld formulation, $2\cos\theta$. At first glance the new factor, identified as B in Figure 2, seems to be a corrected Fresnel-Kirchhoff factor, identified as A in Figure 2. But in the paraxial approximation,

$$\cos\theta \approx 1 - \frac{\theta^2}{2} \quad ; \quad \sin\theta \approx \theta \quad (56)$$

the Rayleigh-Sommerfeld factor, designated C in Figure 2, is identical with factor B. The closeness of the curves for B and C suggests that the scalar integral equations, Eqs (35) and (38), may be reducible to the Rayleigh-Sommerfeld equation, Eq (17).

Derivation of Rayleigh-Sommerfeld Equation

Consider again the case of an initial field propagating predominantly in the +z direction. As shown above, Q_- and P_+ are negligible in this case. Since curve B and curve C in Figure 2 are so close, we use the paraxial approximation of Eq (56) and write E_x by substitution of Eq (35) into Eq (41):

$$E_x = \frac{vk}{4} \int_{S'} \{ (Q_+ - P_-) (2 - \theta^2) + [Q_+ e^{2i\delta} - P_- e^{-2i\delta}] \frac{\theta^2}{2} \} \phi \, dS' \quad (57)$$

Since the term $(2 - \theta^2)$ can be replaced by $2\cos\theta$, and a more rigid angular restriction is made such that the terms containing $\frac{\theta^2}{2}$ are negligible, then the above equation can be written as Eq (58).

$$E_x = ik \int_{S'} E_x' (2\cos\theta) \phi \, dS' \quad (58)$$

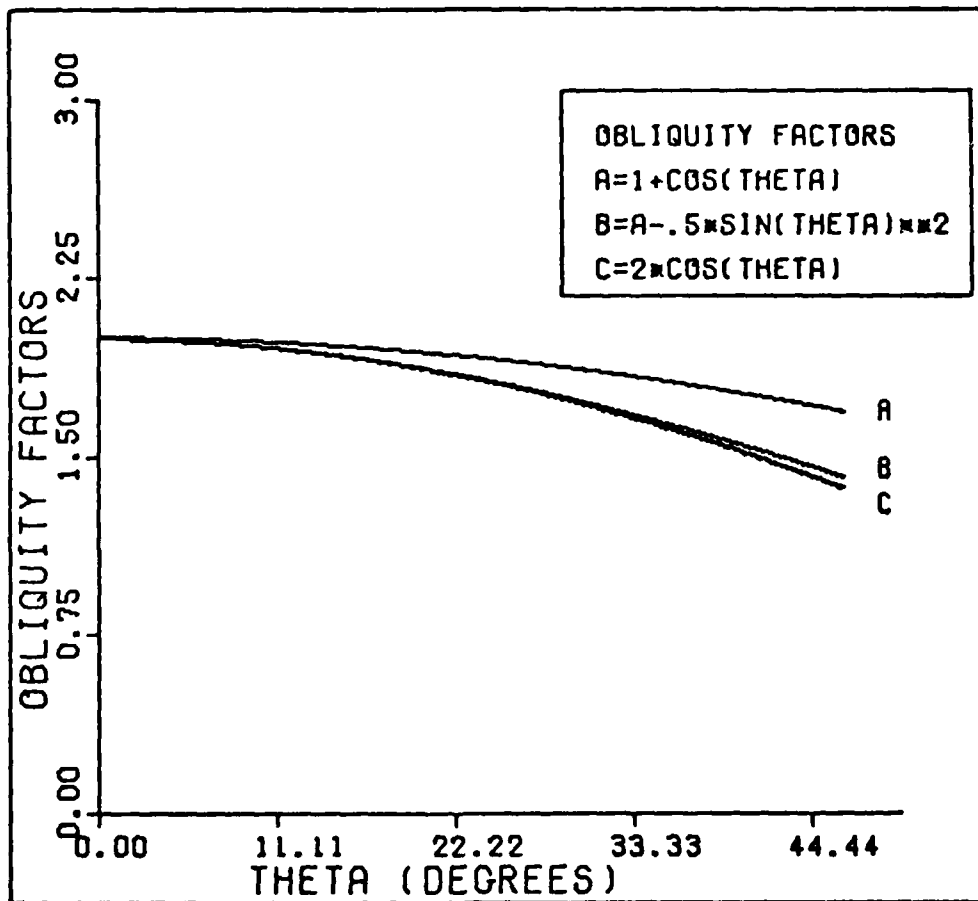


Figure 2. Plot of Various Obliquity Factors where $A = 1 + \cos\theta$, $B = A - \frac{1}{2}\sin^2\theta$, and $C = 2\cos\theta$.

This is the Rayleigh-Sommerfeld equation, Eq (17), if the scalar wave function $u(\vec{r})$ is associated with E_x . A similar equivalence is found for E_y , showing that the Rayleigh-Sommerfeld equation can be accurately applied to the transverse components of the initial field, provided that (1) the initial field is valid EM field, (2) $k \gg 1/R$, (3) $k = k_z$, and (4) the angle θ is small. This last restriction, termed the near-axial approximation, can be stated as $\theta \ll 1$ rad. Yet, even this approximation is not overly restrictive for most applications. This derivation indicates why the scalar diffraction theory is an accurate representation for the transverse components in the near axial region. The examples in Section IV will illustrate how the complex field vector approach is applied to three different polarization states, as well as illustrate that it yields results identical to those predicted by scalar diffraction theory.

IV. Application of the Complex Field Vector Approach

The goal of this section is to illustrate how useful the complex field vector approach is in solving diffraction problems. We begin with some comments on methodology and other topics common to the three examples used in this section. The three examples are then presented, beginning with a linearly polarized field and followed by fields of azimuthal and circular polarizations. The section concludes with some observations on the application of the complex field vector approach to diffraction problems.

Preliminary Comments

As noted in Section III, the initial \bar{E} and \bar{H} are specified on surface S' . In each example in this section, the initial fields are chosen so that the fields are zero at the edge of S' . This boundary condition eliminates the need to consider edge currents. The propagation vector of the initial field is assumed to be $\bar{k} = k_z \hat{a}_z$, so that the field is initially traveling in a predominantly $+z$ direction. In each example, a characteristic scalar, F_{\pm} , is obtained that is proportional to the term $(k \pm k_z)$. If the area S' has a minimum dimension that is at least several wavelengths in size, then F_- can be neglected in comparison to F_+ , simplifying the analysis. The first example will show this comparison in detail. Further, each

example will be solved by using the far field approximation which is valid when the area of S' , denoted as A^2 , is related to the wavelength and distance to the observation plane, z , by Eq (59).

$$\frac{A^2}{\lambda z} \ll \frac{\pi}{2} \quad (59)$$

The area A^2 is interpreted as either the area of a diffracting aperture or the cross-sectional area of a field of finite extent. The far field approximation restricts the proximity of S with respect to S' for a given area A^2 . For the calculations in this section, the dimensions of S' are all on the order of several microns, the wavelength is chosen to be 0.6 microns, and the distance to S is chosen to be one meter. For these parameters, the far field approximation is valid. For the normally incident fields considered here ($\bar{k} = k \hat{a}_z$), most of the energy in the resultant field is expected to be near the axis. So, we also make the axial approximation that $\theta = 0^\circ$. These approximations not only simplify the calculations, but in each example the resultant field is then proportional to either a Fourier transform or a Fourier-Bessel transform of the initial field. For the initial fields chosen here, the transforms are solved in closed form and the resultant irradiance patterns are illustrated. Finally, the Rayleigh-Sommerfeld equation is

used for each example to demonstrate the equivalence discussed at the end of Section III. Let us then begin by discussing the linearly polarized field, \bar{E}_1 .

Example 1: Linear Polarization

The Solution. Consider the field defined by

$$\bar{E}_1 = \begin{cases} \cos \frac{\pi x'}{2a} \cos \frac{\pi y'}{2b} e^{-ik_z z'} \hat{a}_x & \text{on } S' \\ 0 & \text{everywhere else} \end{cases} \quad (60)$$

where S' is the rectangular surface defined by $|x| \leq a$ and $|y| \leq b$. Figure 3 shows the normalized irradiance pattern for \bar{E}_1 where $a = 1.2 \mu\text{m}$ and $y = 0$. The magnetic field is found with Maxwell's equations. Using the definitions of \bar{Q} and \bar{P} as expressed in Eqs (18) and (19), and noting that specializing for S' , $z' = 0$, the initial field is represented by

$$Q_{\pm}' = iF_{\pm} E_x' \quad (61)$$

$$P_{\pm}' = -iF_{\pm} E_x' \quad (62)$$

$$Q_z' = P_z' = \frac{i\pi}{2\omega b} \sin \frac{\pi y'}{2b} \cos \frac{\pi x'}{2a} \quad (63)$$

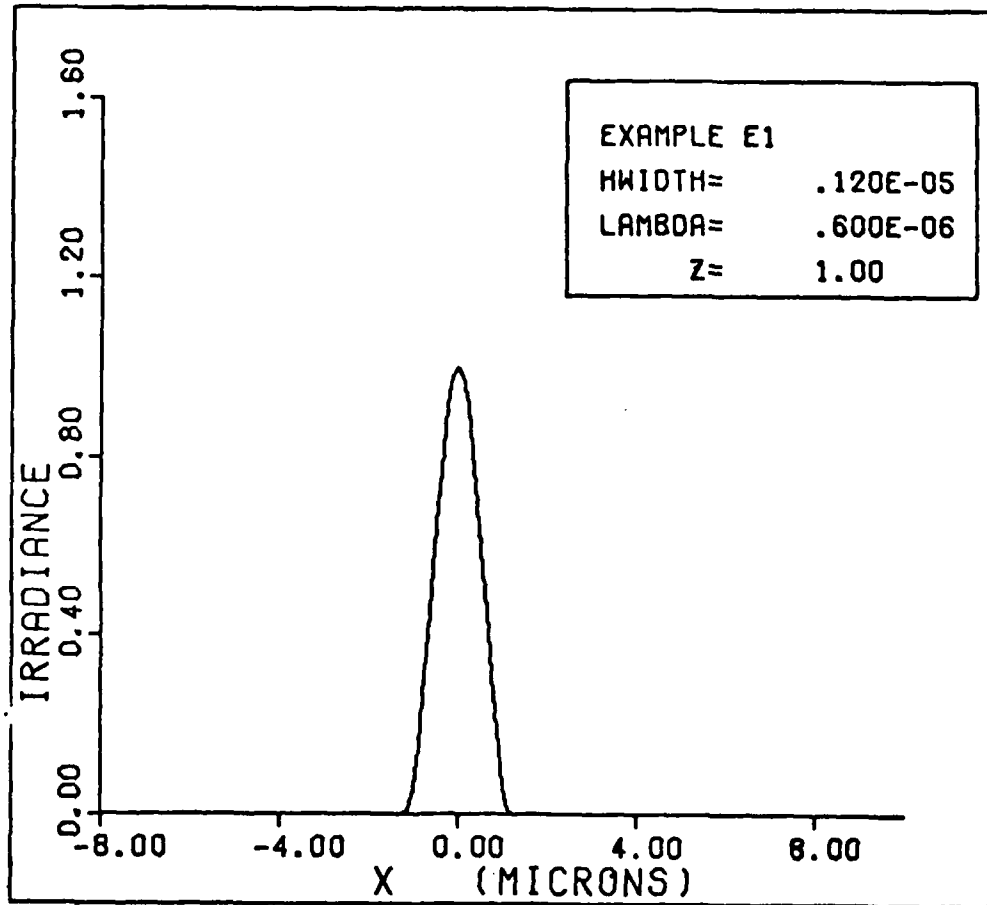


Figure 3. Normalized Irradiance Pattern for Initial E_1 with $a=1.2 \mu\text{m}$, $\lambda=0.6 \mu\text{m}$, and $z=1 \text{ m}$.

where

$$F_{\pm} = \frac{1}{\omega} (k \pm k_z) \quad (64)$$

for

$$k^2 = k_z^2 + \left(\frac{\pi}{2a}\right)^2 + \left(\frac{\pi}{2b}\right)^2$$

and

$$E_{x'} = \begin{cases} \cos \frac{\pi x'}{2a} \cos \frac{\pi y'}{2b} & |x'| \leq a, |y'| \leq b \\ 0 & \text{elsewhere} \end{cases} \quad (65)$$

Since we assumed $\bar{k} = k_z \hat{a}_z$, $k_z^2 \gg \frac{\pi^2}{4} \left(\frac{1}{a^2} + \frac{1}{b^2}\right)$ and the ratio of F_- to F_+ can be expressed as

$$\frac{F_-}{F_+} \approx \frac{\lambda^2}{64} \left[\frac{1}{a^2} + \frac{1}{b^2}\right] \quad (66)$$

For $a \geq \lambda$ and $b \geq \lambda$, the terms containing F_- can be neglected when compared to terms containing F_+ . Neglecting these terms, and making the approximation discussed earlier that $\theta \approx 0^\circ$, one finds that only the Q_+ and P_- integral equations, Eqs (35) and (39), are significant: (See Appendix D)

$$Q_+ = -P_- = -2 F_+ k \int_{S'} E'_x \phi \, dS' \quad (67)$$

Under the far field approximation discussed earlier, the integral can be written as two Fourier transforms that have closed form representations. So the resultant field is expressed as Eq (68).

$$\bar{E}_1(\bar{r}) = -\frac{i}{\lambda z} e^{-ikz} e^{-\frac{ik}{2z}(x^2+y^2)} \frac{\pi^2}{4ab} \times \frac{\cos(\frac{kxa}{z}) \cos(\frac{kxb}{z}) a_x}{[(\frac{\pi}{2a})^2 - (\frac{kx}{z})^2][(\frac{\pi}{2b})^2 - (\frac{ky}{z})^2]} \hat{a}_x \quad (68)$$

This field has the same polarization as the initial field. When the arbitrary assumption is made that the components of the initial field can be treated separately with the Rayleigh-Sommerfeld approach, the same resultant field is obtained for $\theta = 0^\circ$. (See Appendix D)

Utility of the Fast Fourier Transform. In the derivation of Eq (68), the Fourier transform in Eq (69) was obtained for the integral of x' components of the initial field.

$$F(f_x) = \int_{-\infty}^{\infty} T(x') \cos \frac{\pi x'}{2a} e^{-i2\pi f_x x'} dx' \quad (69)$$

where $T(x') = 1$ for $|x'| \leq a$ and is zero elsewhere, and the spatial frequencies are $f_x = \frac{x}{\lambda z}$. The integral can be solved in closed form as

$$F(f_x) = \frac{\pi}{2a} \frac{\cos(2\pi a f_x)}{[(\frac{\pi}{2a})^2 - f_x^2]} \quad (70)$$

An alternate approach to evaluating the integral in Eq (69) is by numerical computation. Let us begin by reviewing some essentials. The continuous Fourier transform (CFT) pair are shown in Eqs (71) and (72).

$$f(x) = \int_{-\infty}^{\infty} F(f_x) e^{i2\pi f_x x} df_x \quad (71)$$

$$F(f_x) = \int_{-\infty}^{\infty} f(x) e^{-i2\pi f_x x} dx \quad (72)$$

The discrete Fourier transform (DFT) is an approximation to the CFT that allows numerical calculation of the transforms. The discrete Fourier transforms pair is (Ref 17:41)

$$f(k) = \sum_{j=0}^{N-1} F(j) e^{i2\pi \frac{jk}{N}}, \quad k=0,1,\dots,N-1 \quad (73)$$

$$F(j) = \frac{1}{N} \sum_{k=0}^{N-1} f(k) e^{-i2\pi \frac{jk}{N}}, \quad j=0,1,\dots,N-1 \quad (74)$$

where k are spatial values, j are spatial frequencies and N is the number of sample points taken of the function in the summation. Direct summation of the DFT requires a time proportional to N , while the use of a Fast Fourier Transform (FFT) reduces this computation to a time proportional to $N \log_2 N$ (Ref 18:70). The FFT routine used for this report was a library routine in the International Mathematics and Statistics Library (IMSL).

For this example, the resultant field was calculated using both the FFT routine and the analytic expression which permits the comparison of the DFT with the CFT. In this comparison, an important tradeoff is made between the distance over which the initial field is sampled (the data window) and the number of sample points taken in this window. Note that the data window must at least cover the non-zero portion of the initial field, but may extend beyond this

region, giving a finite approximation to the actual geometry. In the discrete case, the spatial point x_i that corresponds to a given spatial frequency f_{x_i} is given by

$$x_i = (i) \left(\frac{\lambda Z}{L}\right) \quad i=0,1,\dots,N-1 \quad (75)$$

where L is the length of the data window (Ref 19). So, for a given N , the resolution of the resultant field, which is inversely related to the range of x_i , increases as L increases. But the comparison for this example showed that (1) for fixed N , the maximum percent difference between the CFT and DFT values increased as L increased, and (2) for fixed L , the maximum percent difference decreased with increasing N . One concludes that the resolution must be traded against an accurate representation when using the DFT to compute the resultant field.

Figure 4 shows the normalized irradiance pattern for the resultant field using the FFT routine. Here, $N = 128$ and $L = 12a$. The maximum percent difference between this result and the normalized irradiance pattern predicted by Eq (70), shown in Figure 5, is 1.08 percent. The average percent difference is about 0.05 percent. Thus, the DFT did serve as an accurate approximation to the analytical result for this example.

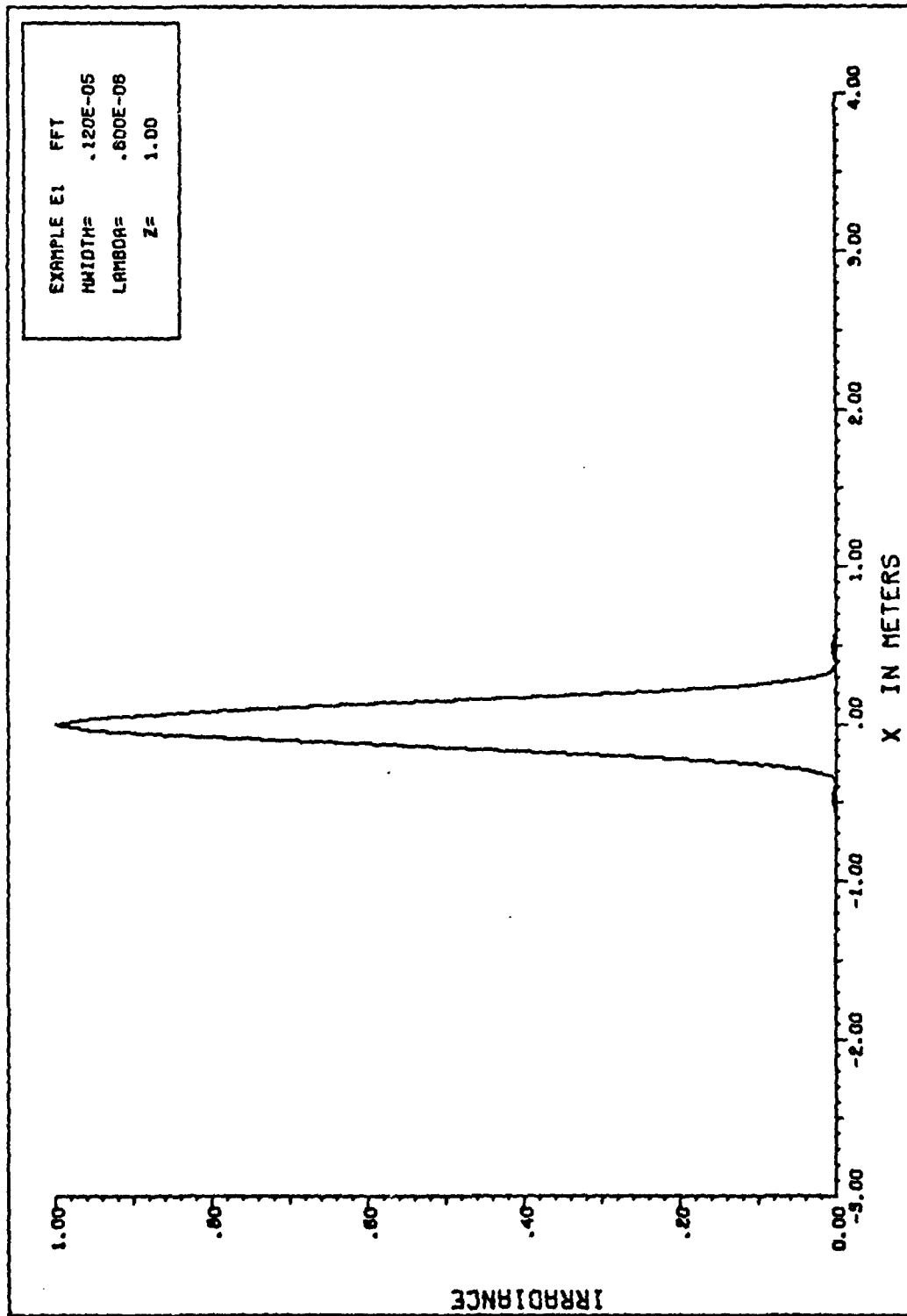


Figure 4. Normalized Irradiance Pattern for Resultant E_1 Using the Fast Fourier Transform.

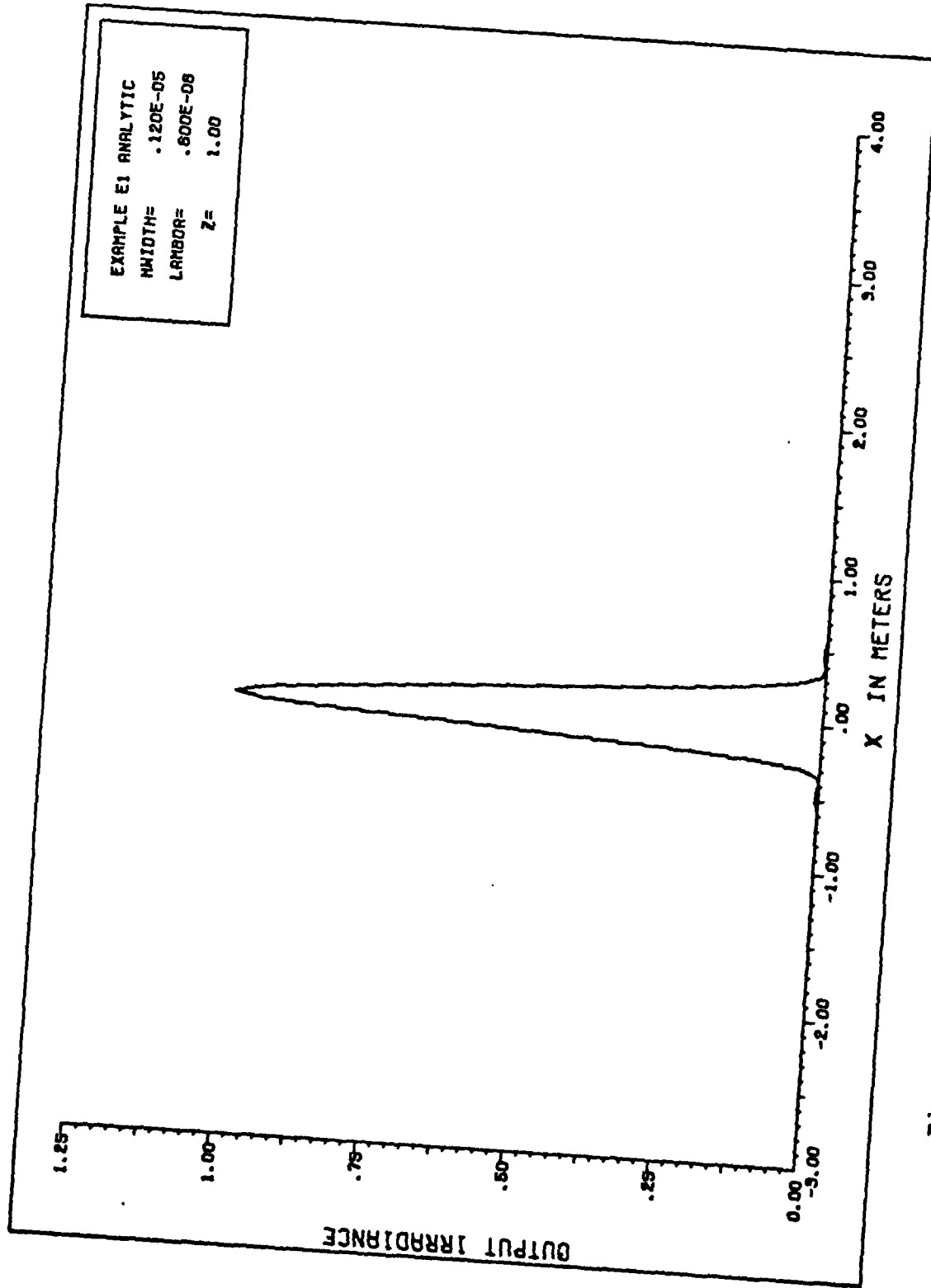


Figure 5. Normalized Irradiance Pattern for Resultant E₁ Using the Analytic Solution.

Example 2: Azimuthal Polarization

Consider the initial field represented by

$$\bar{E}_2 = \begin{cases} -k_\rho J_1(k_\rho \rho) e^{-ik_z z} \hat{a}_\phi & \text{for } \rho \leq a \\ 0 & \text{for } \rho > a \end{cases} \quad (76)$$

where a is the radius of a circular aperture and $k_\rho a = 3.831705970$ (second zero of $J_1(k_\rho \rho)$). Figure 6 shows a sketch of the normalized irradiance for an aperture with a 6 μm radius. Using \bar{E}_2 and the corresponding \bar{H}_2 obtained from Maxwell's equation, \bar{Q}' and \bar{P}' are written on the surface S' . These can be written in component form as shown in Eqs (77) through (79).

$$Q'_\pm = F_\pm e^{\pm i\tau'} J_1(k_\rho \rho') \quad (77)$$

$$P'_\pm = F_\pm e^{\pm i\tau'} J_1(k_\rho \rho') \quad (78)$$

$$Q'_z = P'_z = -\frac{ik_\rho^2}{\omega} J_0(k_\rho \rho') \quad (79)$$

where the characteristic scalar is

$$F_\pm = \frac{k_\rho}{\omega} (k_z \pm k) \quad (80)$$

and

$$k^2 = k_z^2 + k_\rho^2 \quad (81)$$

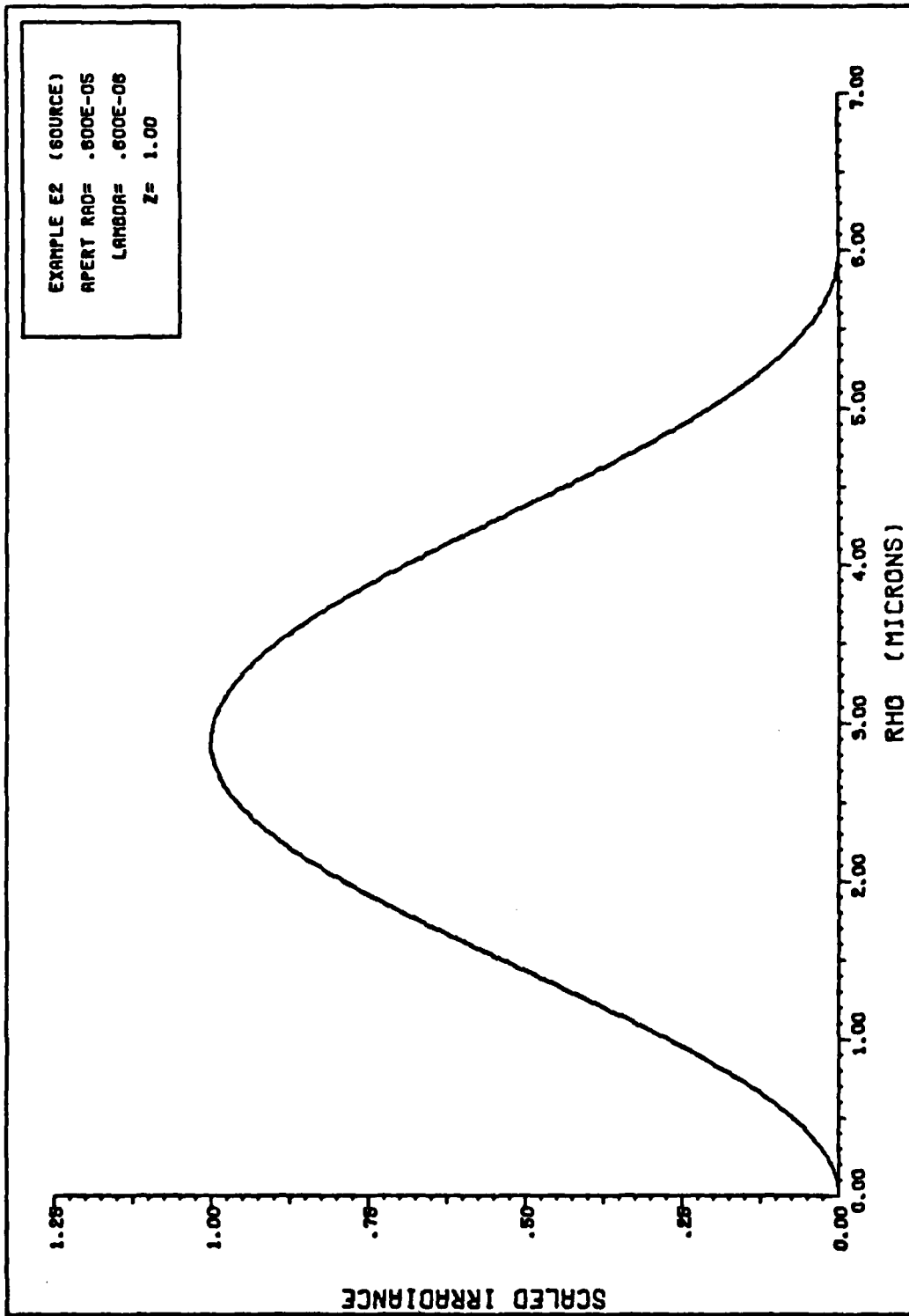


Figure 6. Normalized Irradiance Pattern for Initial E_2 with $a=6 \mu\text{m}$, $\lambda=0.6 \mu\text{m}$, and $z=1\text{m}$.

By an argument similar to that made for the previous example, terms containing F_- are neglected in comparison with terms containing F_+ when a is on the order of a wavelength or greater. By using the six scalar integral equations, Eqs (35) through (40), with the far field approximation, and assuming $\theta \approx 0^\circ$; the resultant field is

$$\bar{E}_2 = -\hat{a}_\phi \frac{2\pi a}{\lambda z} e^{-ikz} e^{-\frac{ik\rho^2}{2z}} \frac{J_1\left(\frac{ka\rho}{z}\right) J_0(k_\rho a)}{\left[\left(\frac{k_\rho}{k_z}\right)^2 - 1\right]} \quad (82)$$

which is of the same polarization as the initial field. The Rayleigh-Sommerfeld equation yields the same result if one assumes the transverse rectangular components of \bar{E}_2 can be treated independently. (See Appendix E) Figure 7 shows the resultant field for $a = 6 \mu\text{m}$.

Example 3: Circular Polarization

Owing to the circular nature of Q_\pm and P_\pm , this example is quite straightforward. Consider the right circularly polarized initial field

$$\bar{E}_3 = \begin{cases} J_0(k_\rho \rho) e^{-ik_z z} \hat{a}_+ & \text{for } \rho \leq a \\ 0 & \text{for } \rho > a \end{cases} \quad (83)$$

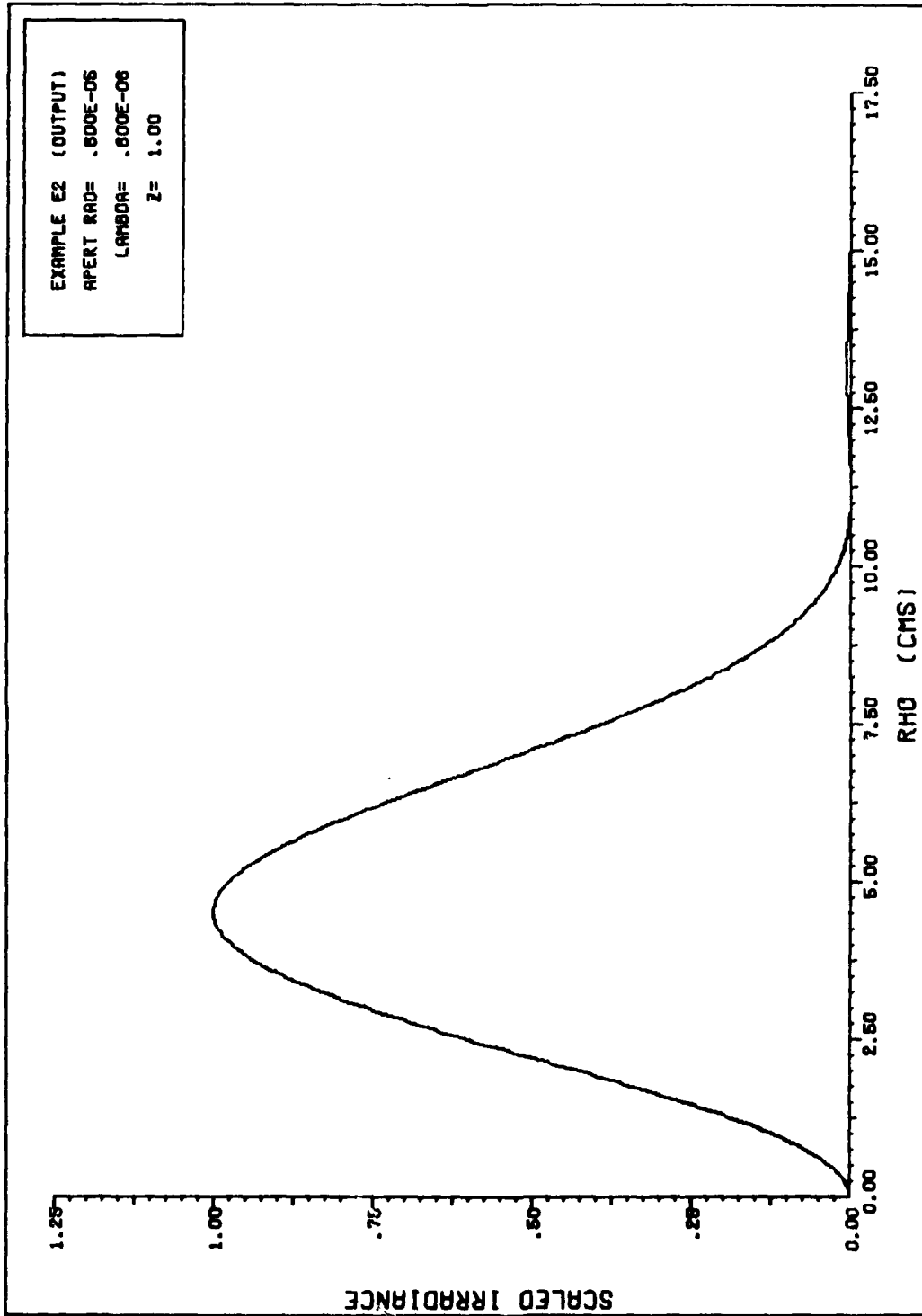


Figure 7. Normalized Irradiance Pattern for Initial E_2 .

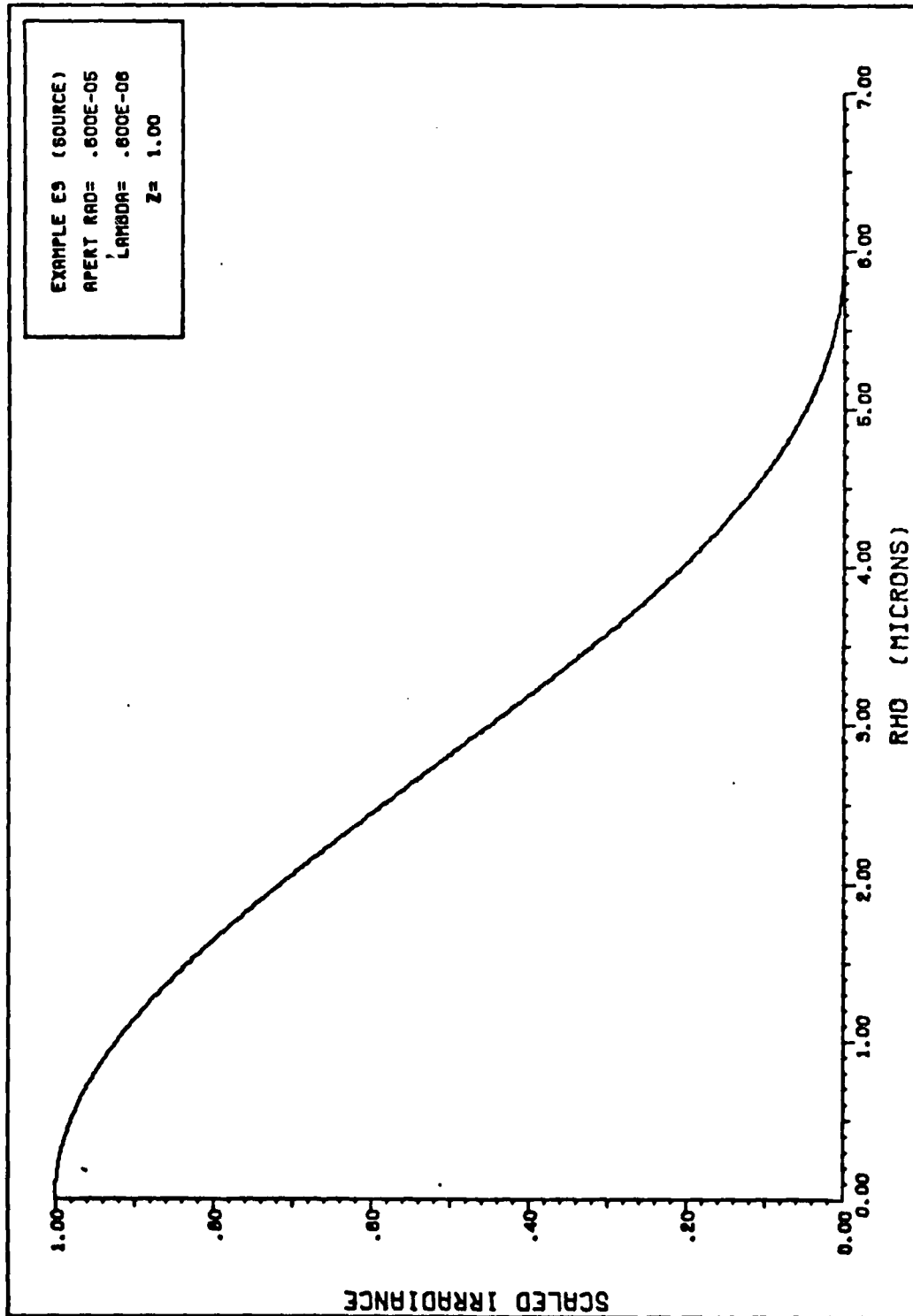


Figure 8. Normalized Irradiance Pattern for Initial \bar{r}_3 with $a=6 \mu\text{m}$, $\lambda=0.6 \mu\text{m}$, and $z=1 \text{ m}$.

where a is the radius of the aperture and $k_{\rho} a = 2.4048255577$ (first zero of $J_0(k_{\rho} \rho)$). Figure 8 shows the normalized initial irradiance for $a = 6$ microns. Then on S' , $Q'_+ = 0$ and $P'_+ = 0$ exactly, and

$$Q'_- = \sqrt{2} i F_- J_0(k_{\rho} \rho') \quad (84)$$

$$P'_- = -\sqrt{2} i F_+ J_0(k_{\rho} \rho') \quad (85)$$

$$Q'_z = P'_z = -\frac{i k_{\rho}}{\sqrt{2} \omega} J_1(k_{\rho} \rho') (\cos \phi' - \sin \phi') \quad (86)$$

where

$$F_{\pm} = \frac{1}{\omega} (k \pm k_z)$$

Again,

$$k^2 = k_z^2 + k_{\rho}^2 \quad (81)$$

since cylindrical coordinates are used. Recall that for $+z$ propagation, P_- and Q_- have a right circular nature as reflected here. Again, the F_+ terms dominate the F_- terms and, using the six integral equations (Eqns (35) through (40)) with the far field approximations and letting $\theta = 0^\circ$, the resultant field is

$$E_3 = \frac{2\pi i a J_1(k_\rho a)}{\lambda z k_\rho} e^{-ikz} e^{-\frac{ik_\rho^2 z}{2}} \frac{J_0\left(\frac{k_\rho a}{z}\right)}{\left[\left(\frac{k_\rho}{zk_\rho}\right)^2 - 1\right]} \hat{a}_+ \quad (87)$$

which is a right circularly polarized field. The normalized irradiance pattern for this field with $a = 6 \mu\text{m}$ is shown in Figure 9. By using Eq (54) and applying the Rayleigh-Sommerfeld equation to each transverse rectangular component, Eq (87) is obtained. (See Appendix F)

Observations on Applications

The methodology is straightforward: (1) form \bar{Q} and \bar{P} from \bar{E} and \bar{H} , (2) use the component equations to obtain the resultant \bar{Q} and \bar{P} , and (3) reform \bar{E} and \bar{H} . The results agree with scalar diffraction theory in the far field approximation and for $\theta \approx 0^\circ$, provided the scalar theory is applied to the transverse rectangular components. Notice that, by assuming $\theta \approx 0^\circ$, the possibility of any off-axis power flow is eliminated since the scalar integrals that could contribute to such power flow depend directly on θ . The possibility of polarization shifts for the off-axis region is similarly negated. An example of such a polarization shift would be the development of a \hat{a}_y or \hat{a}_z component in the resultant field of example 1. Thus, the complex field vector approach clearly indicates that

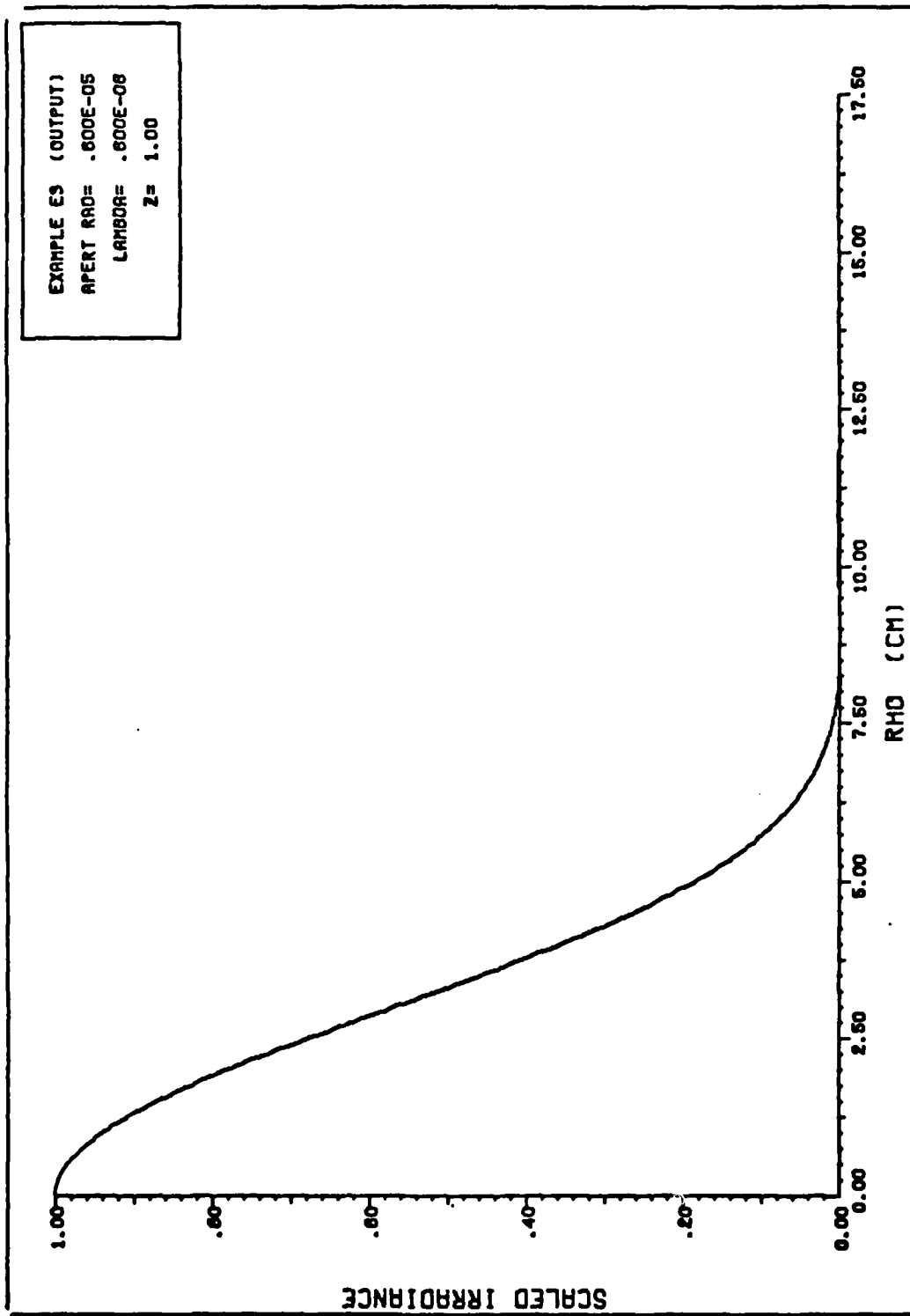


Figure 9. Normalized Irradiance Pattern for Resultant E_3 .

scalar theory can be used under the far field approximation and for $\theta = 0^\circ$.

The characteristic scalar, F_{\pm} , not only simplifies the application, but gives insight into the diffraction process. If the aperture is smaller than two wavelengths in size, the F_{\pm} terms could not be neglected, and the resultant field would be changed accordingly. This could give rise to other polarizations and change the amount or direction of power flow.

Finally, the application of this approach is straightforward since, once \bar{Q} and \bar{P} are formed, the resultant field is obtained from a set of component equations. The application is particularly straightforward for circular polarization problems, as seen in example 3. This approach avoids the necessity of resolving the initial \bar{E} into rectangular components as required when using scalar diffraction theory. However, since this approach agreed with scalar diffraction theory under the axial and far field approximations, and since the scalar theory was shorter in application, applications in this region are more quickly accomplished with scalar theory without any loss of accuracy. If either approximation is not valid, the complex field vector approach, though more lengthy in application, is more appropriate than the scalar theory. So, this approach is not only rigorous in its development as shown in Section III, but it is applied in a straightforward manner as demonstrated in this section.

V. Conclusions and Recommendations

In this section, three important conclusions and four major recommendations are discussed. As a brief summary, recall that the use of the complex field vectors led to uncoupled field equations. Then these equations were solved by rewriting the results obtained by Doughty in terms of \bar{Q} and \bar{P} . The resultant field was expressed at this point by a pair of uncoupled vector integrals over the open surface S' . When S' was planar, the resultant field was written in terms of six component integrals over S' . Section IV considered three examples that showed how easily these integrals are applied. In the special case where (1) $\bar{k} = k \hat{a}_z$ initially, and (2) $\theta \ll 1$ rad, the tangential components of the resultant field were expressed in a form identical to the Rayleigh-Sommerfeld equation. With this summary in mind, the following conclusions are presented.

Conclusions

First, the objectives set forth in Section I have been met in this report. The complex field vector approach leads to two separated vector integral equations, Eqs (24) and (25), that are evaluated over an open surface S' . The only restrictions on these equations are the assumptions that Ohm's Law holds in the medium and that the medium is homogeneous, isotropic, linear and free of charge, and the

requirement that the initial \bar{E} and \bar{H} must satisfy Maxwell's equations on S' . When S' is specialized to be a plane surface, the six component integrals in Eqs (35) through (40) were derived by the further restriction that $k \gg 1/R$. Thus, the development of resultant field is rigorous, as is required for an acceptable vector diffraction theory. This approach has the further advantage that the application is mathematically simple, since only separated component integrals are involved. Indeed, for the special case where $\bar{k} = k \hat{a}_z$ initially and $\theta \ll 1$ rad, the scalar equations express the transverse components of the resultant \bar{E} in a form identical to the Rayleigh-Sommerfeld equation. So the complex field vector approach can be as simple and straightforward as scalar diffraction theory.

Second, this derivation of the Rayleigh-Sommerfeld equation explains why this equation accurately describes the near-axial irradiance pattern. It further implies that the Rayleigh-Sommerfeld equation is not accurate in the region farther off the axis. In this region, the set of scalar integral equations should be used. Thus, the complex field vector approach is clearly more general than scalar diffraction theory.

Third, the applications discussed in Section IV provide insight into the diffraction process. The characteristic scalar F_{\pm} that occurred in the three examples describes the effect of the aperture size on when terms in F_{-} could be neglected by comparison to terms in F_{+} . Also, the

circularly polarized nature of Q_{\pm} and P_{\pm} that was discussed in Section III is strongly evident in the third example which dealt with a circularly polarized initial field. Further, it is important to note that the terms that could have caused polarization shifts and off-axis power flow were eliminated only by the angular restrictions and not inherently by the component integrals. Finally, the restriction that $\theta \approx 0^{\circ}$ removed the terms containing δ . (Recall that $\delta = \tan^{-1} \left(\frac{x-x'}{y-y'} \right)$. The ratio of coordinates relates field values at a point on the initial field to the value of the field at an observation point, which gives a certain orientation between initial and resultant fields.) So it is not surprising that the results agree exactly with the predictions of scalar diffraction theory.

Based on these three main conclusions, the following recommendations are made.

Recommendations

First, the calculation of off-axis power flow and polarization shifts needs to be developed more fully. Using the Fresnel approximation in place of the far field approximation casts the component integrals in the form of two dimensional convolutions. These equations may be amenable to fast Fourier transform techniques if the initial field is chosen properly. The resulting components of \bar{Q} and \bar{P} would then be used to form \bar{E} and \bar{H} as well as the Poynting vector $\bar{S} = \bar{E} \times \bar{H}$. From these three

quantities, the time average polarizations and power flow can be studied.

Second, the sensitivity of this approach to the requirement that the initial \bar{E} and \bar{H} satisfy Maxwell's equations on S' should be assessed. For example, if only the initial transverse components of \bar{E} and the direction of propagation were known, some information about the resultant field may still be obtained by partially forming \bar{Q} and \bar{P} . A weakening of the above requirement would make the results more useful in practical applications.

Third, an example should be worked where the field is discontinuous at the edge of the surface S' , so that an edge current is introduced in order to satisfy Maxwell's equations on S' . The example would illustrate how to deal with these fields. The resultant field should be compared against the field predicted by the Rayleigh-Sommerfeld equation to assess the effect of edge currents on diffraction.

Fourth, the term δ discussed in the third conclusion should be investigated. If the initial field is azimuthally symmetric, δ would seem less significant since the spatial phase shift should also be azimuthally symmetric. Also, the ratio of coordinates $\frac{x-x'}{y-y'}$ is not unique for each set of points described by $r-r'$. This mapping should be investigated to develop more clearly the nature of δ .

Throughout this report it has been emphasized that the diffraction problem has been solved by the complex field vector approach in a manner that is both rigorous and

mathematically simple. Other solutions to the diffraction problem exist, some more useful than others. Unfortunately, the most useful (scalar diffraction theory) is the least rigorous and the more rigorous approaches are sufficiently complex as to be less useful. The complex field vector approach spans the "middle ground" of being derived directly from Maxwell's equations and being useful in obtaining both solutions and insight into diffraction problems.

Bibliography

1. Sommerfeld, A., "Mathematische Theorie der Diffraction." Math. Ann., 47: 317 (1896).
2. Kottler, F., "Electromagnetische Theorie der Beugung an Schwarzen Schermen." Ann. Physik, 71: 457 (1923).
3. Schelkunoff, S.A., "On Diffraction and Radiation of Electromagnetic Waves." Phys. Rev., 56: 308 (1939).
4. Stratton, J.A. and Chu, L.J., "Diffraction Theory of Electromagnetic Waves." Phys. Rev., 56: 99 (1939).
5. Bouwkamp, C.J., "Diffraction Theory." Reports on Progress in Physics, 27: 35 (1954).
6. Stratton, J.A., Electromagnetic Theory. New York: McGraw-Hill Book Co., 1941.
7. Doughty, G.R., "Theoretical Analysis of Resonator Modes in the Presence of Homogeneous Media." PhD Dissertation, School of Engineering, Air Force Institute of Technology, Wright-Patterson AFB OH, May 1977.
8. Born, M. and Wolf, E., Optics, 5th Edition, Oxford: Pergamon Press, 1975.
9. Baker, B. and Copson, E., Huygen's Principle, 2d Edition, Oxford: Clarendon Press, 1950.
10. Goodman, J.W., Fourier Optics, San Francisco: McGraw-Hill Book Co., 1968.
11. Silver, S., "Microwave Aperture Antenna and Diffraction Theory." Journal of Optical Society of America, 52: 131 (1962).
12. Andrews, C.L., "A Correction to the Treatment of Fresnel Diffraction." American Journal of Physics, 19: 280 (1951).
13. Bateman, H., Mathematical Analysis of Electrical and Optical Wave-motion. New York: Dover Publications, 1955.
14. Silberstein, L. "Elektromagnetische Grundgleichungen in Bivektorieller Behandlung." Ann. Physik, 22: 579 (1907).

15. Doughty, G.R., Deputy Department Head, Department of Physics, Air Force Institute of Technology. (Private conversations.) Wright-Patterson AFB OH, May-August 1979.
16. Harrington, R.F., Time Harmonic Electromagnetic Fields, New York: McGraw-Hill Book Co., 1961.
17. Bergland, G.D., "A Guided Tour of the Fast Fourier Transform." IEEE Spectrum, 6, No. 7, 41-52 (July 1969).
18. Brigham, E.O. and Morrow, R.E., "The Fast Fourier Transform." IEEE Spectrum, 4, No. 12, 63-70 (Dec 1967).
19. Shankland, D.G., Professor, Department of Physics, Air Force Institute of Technology. (Private conversation.) Wright-Patterson AFB OH, 6 August 1979.

Appendix A

Components of the Vector Integral Equation for \bar{Q}

The purpose of this appendix is to obtain Eq (26) from Eq (24). Let us begin by recalling Eq (24).

$$\bar{Q}(\mathbf{r}) = \int_{S'} \{ [\hat{\mathbf{n}}\bar{Q}'(\bar{\mathbf{r}}')] \cdot \nabla \times \bar{\mathbf{G}} + \frac{1}{K} [\hat{\mathbf{n}}\bar{Q}'(\bar{\mathbf{r}}')] \cdot \nabla \times \nabla' \times \bar{\mathbf{G}} \} dS' \quad (\text{A.1})$$

Letting $\hat{\mathbf{n}}\bar{Q}'(\bar{\mathbf{r}}') = \mathbf{J}(\bar{\mathbf{r}}')$, this equation can be written as

$$\bar{Q} = \int_{S'} \{ \nabla \times [\mathbf{J} \cdot \bar{\mathbf{G}} + \frac{1}{K} \mathbf{J} \cdot \nabla' \times \bar{\mathbf{G}}] \} dS' \quad (\text{A.2})$$

Recalling that $\bar{\mathbf{G}} = \bar{\mathbf{I}}\phi$, one readily finds that $\nabla' \times \bar{\mathbf{G}}$ is the completely asymmetric dyad,

$$\nabla' \times \bar{\mathbf{G}} = \begin{pmatrix} 0 & \phi_{,z} & -\phi_{,y} \\ -\phi_{,z} & 0 & \phi_{,x} \\ \phi_{,y} & -\phi_{,x} & 0 \end{pmatrix} \quad (\text{A.3})$$

where $\phi_{,z} \equiv \frac{\partial \phi}{\partial z}$, etc. Then by direct manipulation, one has

$$\begin{aligned}
\nabla \times (\mathbf{J} \cdot \nabla \times \bar{\mathbf{G}}) &= \hat{\mathbf{a}}_x [J_y \phi_{,xy} + J_z \phi_{,xz} - J_x (\phi_{,yy} + \phi_{,zz})] \\
&+ \hat{\mathbf{a}}_y [J_z \phi_{,yz} + J_x \phi_{,yx} - J_y (\phi_{,xx} + \phi_{,zz})] \\
&+ \hat{\mathbf{a}}_z [J_x \phi_{,zx} + J_y \phi_{,zy} - J_z (\phi_{,xx} + \phi_{,yy})] \quad (\text{A.4})
\end{aligned}$$

Observing that $\bar{\mathbf{J}} \cdot \bar{\mathbf{G}} = \bar{J} \phi$, the other term in the integrand is written in component form as

$$\begin{aligned}
\nabla \times \bar{J} \phi &= \hat{\mathbf{a}}_x (J_z \phi_{,y} - J_y \phi_{,z}) \\
&+ \hat{\mathbf{a}}_y (J_x \phi_{,z} - J_z \phi_{,x}) \\
&+ \hat{\mathbf{a}}_z (J_y \phi_{,x} - J_x \phi_{,y}) \quad (\text{A.5})
\end{aligned}$$

Noting that ϕ satisfies the scalar Helmholtz equation, Eq (14), and choosing $\hat{\mathbf{n}} = +\hat{\mathbf{a}}_z$ so that S' is planar and

$$\bar{\mathbf{J}} = -Q_y' \hat{\mathbf{a}}_x + Q_x' \hat{\mathbf{a}}_y \quad (\text{A.6})$$

one obtains for the resultant field

$$\begin{aligned}
\bar{Q} &= \hat{a}_x \int_{S'} \{-Q'_{x\phi,z} - \frac{1}{k}[Q'_{y\phi}(k^2\phi+\phi)_{,xx}) - Q'_{x\phi,xy}]\} dS' \\
&+ \hat{a}_y \int_{S'} \{-Q'_{y\phi,z} - \frac{1}{k}[-Q'_{x\phi}(k^2\phi+\phi)_{,yy}) + Q'_{y\phi,yx}]\} dS' \\
&+ \hat{a}_z \int_{S'} \{Q'_{x\phi,x} + Q'_{y\phi,y} + \frac{1}{k}[Q'_{x\phi,zy} - Q'_{y\phi,zx}]\} dS' \quad (A.7)
\end{aligned}$$

Taking the scalar product of \hat{a}_x with Eq (A.7), Eq (A.8) is obtained:

$$Q_x = \int_{S'} \{-Q'_{x\phi,z} - \frac{1}{k}[Q'_{y\phi}(k^2\phi+\phi)_{,xx}) - Q'_{x\phi,xy}]\} dS' \quad (A.8)$$

This is Eq (26) as desired. Equations (27) and (28) are obtained by the scalar product of Eq (A.7) with \hat{a}_y and \hat{a}_z , respectively.

Appendix B

Derivatives of the Green's Function

This appendix obtains the first and second derivatives of the scalar portion of the dyadic Green's function, $\phi = \exp[-ikR]/4\pi R$. The first derivative with respect to x_i is obtained directly as

$$\phi_{,x_i} = \frac{\partial \phi}{\partial x_i} = - (ik + 1/R) \phi \frac{(x_i - x'_i)}{R} \quad (\text{B.1})$$

where x_i is x for $i = 1$, y for $i = 2$, and z for $i = 3$. The second derivative is more complicated. By the rules for differentiating a product, one has

$$\begin{aligned} \phi_{,x_i x_j} = \frac{\partial}{\partial x_j} \left(\frac{\partial \phi}{\partial x_i} \right) &= - (ik + \frac{1}{R}) \phi \left[\frac{1}{R} \frac{\partial (x_i - x'_i)}{\partial x_j} - \frac{(x_i - x'_i)(x_j - x'_j)}{R^2} \right] \\ &- (ik + \frac{1}{R})^2 \phi \frac{(x_i - x'_i)(x_j - x'_j)}{R^2} \\ &+ \frac{(x_i - x'_i)(x_j - x'_j)}{R^3} \phi \end{aligned} \quad (\text{B.2})$$

Noting that $\frac{\partial (x_i - x'_i)}{\partial x_j} = \delta_{ij}$, and by direct algebraic manipulation,

$$\phi_{,x_i x_j} = -\phi \left\{ \frac{\delta_{ij}}{R} \left(ik + \frac{1}{R} \right) + \frac{(x_i - x'_i)(x_j - x'_j)}{R^2} \left[ik + \frac{2}{R}(ik+1) - k^2 + \frac{1}{R^2} \right] \right\} \quad (\text{B.3})$$

Under the approximation $k \approx 1/R$, Eq (B.1) becomes

$$\phi_{,x_i} = -ik \phi \frac{(x_i - x'_i)}{R} \quad (\text{B.4})$$

and Eq (B.3) becomes

$$\phi_{,x_i x_j} = -ik \phi \frac{\delta_{ij}}{R} - k^2 \frac{(x_i - x'_i)(x_j - x'_j)}{R^2} \quad (\text{B.5})$$

These last two equations are Eqs (29) and (30).

Appendix C

Expression of Complex Component Q_+ Using Impedances

We have the complex component

$$Q_+ = Q_x + i Q_y \quad (C.1)$$

where

$$Q_x = \mu H_x + i\sqrt{\mu\epsilon} E_x \quad (C.2)$$

and

$$Q_y = \mu H_y + i\sqrt{\mu\epsilon} E_y \quad (C.3)$$

Substituting Eqs (C.2) and (C.3) into Eq (C.1), and factoring out the component of \vec{E} ,

$$Q_+ = \sqrt{\mu\epsilon} E_y \left(-1 + \sqrt{\frac{\mu}{\epsilon}} \frac{H_x}{E_y}\right) + i\sqrt{\mu\epsilon} E_x \left(1 + \sqrt{\frac{\mu}{\epsilon}} \frac{H_y}{E_x}\right) \quad (C.4)$$

Using a complex form for the intrinsic impedance,

$$\eta = \sqrt{\frac{\mu}{\epsilon}} \quad (C.5)$$

and defining the wave impedances following Harrington,
(Ref 16:86)

$$\frac{E_x}{H_y} = \pm n_{xy}^{\pm} \quad (C.6)$$

and

$$\frac{E_y}{H_x} = \pm n_{yx}^{\pm} \quad (C.7)$$

where the upper sign is for +z propagation and the lower sign for -z propagation, one obtains the final expression for Q_+ that is Eq (49):

$$Q_+ = -\sqrt{\mu\epsilon} E_y \left(1 \pm \frac{n}{n_{yx}^{\pm}}\right) + i\sqrt{\mu\epsilon} E_x \left(1 \pm \frac{n}{n_{xy}^{\pm}}\right) \quad (C.8)$$

Appendix D

Development of Example 1

This appendix gives a more detailed development of Example 1, where the field was defined by Eq (60). On S' , one has

$$\bar{E}'_1 = \cos \frac{\pi x'}{2a} \cos \frac{\pi y'}{2b} \hat{a}_x \quad (D.1)$$

$$\bar{H}'_1 = \frac{1}{\omega \mu} \hat{a}_y (k_z \cos \frac{\pi x'}{2a} \cos \frac{\pi y'}{2b}) + i \hat{a}_z (\frac{\pi}{2b} \sin \frac{\pi y'}{2b} \cos \frac{\pi x'}{2a}) \quad (D.2)$$

Using the definitions of \bar{Q} and \bar{P} , Eq (18) and (19), and Eq (34), the components of \bar{Q}' and \bar{P}' are

$$Q'_\pm = i F_\pm E'_x \quad (D.3)$$

$$P'_\pm = -i F_\pm E'_x \quad (D.4)$$

$$Q'_z = P'_z = \frac{i\pi}{2\omega b} \sin \frac{\pi y'}{2b} \cos \frac{\pi x'}{2a} \quad (D.5)$$

where

$$F_\pm = \frac{1}{\omega} (k \pm k_z) \quad (D.6)$$

and

$$E'_x = \cos \frac{\pi x'}{2a} \cos \frac{\pi y'}{2b} \quad (D.7)$$

As discussed in Section IV, the F_- terms can be neglected when compared to the F_+ terms for $a \geq \lambda$. Substituting the value in Eq (D.3) into the scalar integral equations, Eqs (35) through (37), and making the paraxial approximation of Eq (56), one finds

$$Q_+ = -k \int_{S'} F_+ (2 - \theta^2) E'_x \phi \, dS' \quad (D.8)$$

$$Q_- = -k \int_{S'} F_- \frac{\theta^2}{2} e^{2i\delta} E'_x \phi \, dS' \quad (D.9)$$

$$Q_z = -\frac{ik}{2} \int_{S'} F_+ (2 - \frac{\theta^2}{2}) e^{i\delta} \theta E'_x \phi \, dS' \quad (D.10)$$

A similar substitution is made using Eq (D.4) for the \bar{P} equations. One should note that all the components of \bar{Q} and \bar{P} are present in the resultant field, so all the components of \bar{E} and \bar{H} are possible. This allows polarization shifts and off axis power flow to occur. Also, note that all the terms containing δ are proportional to θ , so as θ approaches zero, these terms vanish and the sense of orientation represented by δ is lost. Let $\theta = 0^\circ$. Then, for \bar{Q}

$$Q_+ = -F_+ k \int_{S'} E'_x \phi \, dS' \quad (D.11)$$

$$Q_- = Q_z = 0 \quad (D.12)$$

and for \bar{P} ,

$$P_- = -Q_+ \quad (D.13)$$

$$P_+ = P_z = 0 \quad (D.14)$$

The integral in Eq (D.11) is

$$I = \int_{S'} E'_x \phi \, dS' = \int_{-b}^b dy' \int_{-a}^a dx' \cos \frac{\pi x'}{2a} \cos \frac{\pi y'}{2b} \phi \quad (D.15)$$

Under the far field approximation, Eq (59), and since $\theta \approx 0^\circ$, the ϕ term is approximated by

$$\phi = \frac{e^{-ikR}}{4\pi R} \approx \frac{1}{4\pi z} e^{-ikz} e^{-\frac{ik}{2z}(x^2+y^2)} e^{\frac{ik}{z}(xx'+yy')} \quad (D.16)$$

So the integral becomes

$$I = \frac{e^{-ikz}}{4\pi z} e^{-\frac{ik}{2z}(x^2+y^2)} I_x I_y \quad (D.17)$$

where

$$I_x = \int_{-a}^a \cos \frac{\pi x'}{2a} e^{i \frac{k x x'}{z}} dx' \quad (D.18)$$

and similarly for I_y .

Consider the integral I_x . Let x' be $-x'$ and multiply Eq (D.18) by an aperture function $T(x')$ where

$$T(x') = \begin{cases} 1 & |x'| \leq a \\ 0 & |x'| > a \end{cases} \quad (D.19)$$

Then

$$I_x = - \int_{-\infty}^{\infty} [T(x') \cos \frac{\pi x'}{2a}] e^{-i \frac{k x x'}{z}} dx' \quad (D.20)$$

This is the Fourier transform of $[T(x') \cos \frac{\pi x'}{2a}]$,

$$I_x = F\{T(x') \cos \frac{\pi x'}{2a}\} \quad (D.21)$$

which has a closed form solution

$$I_x = \frac{\pi}{2a} \frac{\cos(\frac{k x a}{z})}{[(\frac{\pi}{2a})^2 - (\frac{k x}{z})^2]} \quad (D.22)$$

A similar analysis for I_y yields

$$I_y = \frac{\pi}{2b} \frac{\cos\left(\frac{kyb}{z}\right)}{\left[\left(\frac{\pi}{2b}\right)^2 - \left(\frac{kx}{z}\right)^2\right]} \quad (\text{D.23})$$

So the resultant field is expressed by

$$\bar{E} = -\frac{i\nu}{2} \frac{F_+}{\lambda z} e^{-ikz} e^{-\frac{ik}{2z}(x^2+y^2)} I_x I_y \hat{a}_x \quad (\text{D.24})$$

where Eq (41) was used. Noting that $F_+ = \frac{2}{V}$, one finds

$$\bar{E} = -\frac{i}{\lambda z} e^{-ikz(x^2+y^2)} \frac{\pi^2}{4ab} \frac{\cos\left(\frac{kxa}{z}\right)\cos\left(\frac{kyb}{z}\right)}{\left[\left(\frac{\pi}{2a}\right)^2 - \left(\frac{kx}{z}\right)^2\right]\left[\left(\frac{\pi}{2b}\right)^2 - \left(\frac{ky}{z}\right)^2\right]} a_x \quad (\text{D.25})$$

This is Eq (68).

If one assumes the transverse components of the initial field can be treated independently with the Rayleigh-Sommerfeld equation, Eq (17), then the resultant field is, for $\theta = 0^\circ$ and using the far field approximation,

$$\bar{E} = -\frac{i}{\lambda z} e^{-\frac{ik}{2z}(x^2+y^2)} \int_S \cos\frac{\pi x'}{2a} \cos\frac{\pi y'}{2b} e^{\frac{ik}{z}(xx'+yy')} dS \quad (\text{D.26})$$

This integral is the same one evaluated in Eq (D.15), so the resultant field obtained from scalar diffraction theory is the same as that obtained in Eq (D.25).

Appendix E

Development of Example 2

This appendix gives more details about Example 2, where the field on S' was

$$\bar{E}'_z = -k_\rho J_1(k_\rho \rho') \hat{a} \quad (\text{E.1})$$

$$\bar{H}'_z = \frac{k_\rho k_z}{\omega \mu} J_1(k_\rho \rho') \hat{a} - \frac{ik_\rho^2}{\omega \mu} J_0(k_\rho \rho') \hat{a}_z \quad (\text{E.2})$$

One forms the components of \bar{Q}' and \bar{P}' by using the definitions:

$$Q'_\pm = F_\pm e^{\pm i\phi'} J_1(k_\rho \rho') \quad (\text{E.3})$$

$$P'_\pm = F_\mp e^{\pm i\phi'} J_1(k_\rho \rho') \quad (\text{E.4})$$

$$Q'_z = P'_z = -\frac{ik_\rho^2}{\omega} J_0(k_\rho \rho') \quad (\text{E.5})$$

where

$$F_\pm = \frac{k_\rho}{\omega} (k_z \pm k) \quad (\text{E.6})$$

As argued in Section IV, the F_- terms are neglected in comparison to F_+ terms so long as $a \geq \lambda$. The terms in Eqs (E.3) and (E.4) are substituted into Eqs (35) through

(40). The discussion in Appendix D applies here for the paraxial approximation. Let us proceed immediately by letting $\theta = 0^\circ$. The far field approximation for ϕ in cylindrical coordinates is

$$\phi = \frac{1}{4\pi z} e^{-ikz} e^{-\frac{ik}{2z}\rho^2} e^{+i\frac{k\rho\rho'}{z} \cos(\tau'-\tau)} \quad (\text{E.7})$$

So the resultant field is described by the components

$$Q_+ = \frac{2ikF_+}{4\pi z} e^{-ikz} e^{-\frac{ik\rho^2}{2z}} I_+ \quad (\text{E.8})$$

$$P_- = \frac{2ikF_+}{4\pi z} e^{-ikz} e^{-\frac{ik\rho^2}{2z}} I_- \quad (\text{E.9})$$

$$Q_- = Q_z = P_+ = P_z = 0 \quad (\text{E.10})$$

where

$$I_{\pm} = \int_0^a \rho' d\rho' \int_0^{2\pi} d\phi' e^{\pm i\phi'} J_1(k\rho\rho') e^{i\frac{k\rho\rho'}{z} \cos(\tau'-\tau)} \quad (\text{E.11})$$

The integral in ϕ' is solved first. By using the identity,

$$\int_0^{2\pi} e^{-im\theta} e^{-ia \cos(\theta-\phi)} d\theta = 2\pi(-i)^m e^{-im\phi} J_m(a) \quad (\text{E.12})$$

one finds

$$I_{\pm} = -2\pi i e^{\pm i\phi} \int_0^a \rho' d\rho' J_1(k\rho\rho') J_1\left(\frac{k\rho\rho'}{z}\right) \quad (\text{E.13})$$

where the identities

$$J_{-n}(x) = (-1)^n J_n(x) \quad (\text{E.14})$$

$$J_n(-x) = (-1)^n J_n(x) \quad (\text{E.15})$$

were also useful. With the use of an aperture function like Eq (D.19), the integral in ρ' is a Fourier-Bessel transform (or a Hankel transform of order one) that may be solved in closed form. So the resultant field is

$$\bar{E}_2 = -\hat{a}_\phi \frac{2\pi a}{\lambda z} e^{-ikz} e^{-\frac{ik_\rho^2}{2z}} \frac{J_1\left(\frac{ka\rho}{z}\right) J_0(k_\rho a)}{\left(\frac{k_\rho}{z}\right)^2 - 1} \quad (\text{E.16})$$

where the relation $F_+ = \frac{2k_\rho}{v}$ was used. This is Eq (82).

In order to apply scalar diffraction theory, one must first write the initial field in rectangular coordinates, then the initial field on S' is

$$\bar{E}_2(\bar{r}') = \hat{a}_x [k_\rho J_1(k_\rho \rho') \sin\phi'] - \hat{a}_y [k_\rho J_1(k_\rho \rho') \cos\phi'] \quad (\text{E.17})$$

Then, assume each component can be treated independently with the Rayleigh-Sommerfeld equation, Eq (17), and use the exponential forms of the circular functions,

$$\sin\phi' = \frac{e^{i\phi'} - e^{-i\phi'}}{2i} ; \quad \cos\phi' = \frac{e^{i\phi'} + e^{-i\phi'}}{2} \quad (\text{E.18})$$

Consider the \hat{a}_x component first. Under the far field approximation and letting $\theta = 0^\circ$, the resultant \hat{a}_x component is

$$E_x = -\frac{k_\rho}{2\lambda z} e^{-ikz} e^{-\frac{ik_\rho^2}{2z}} [I_+ - I_-] \quad (\text{E.19})$$

where the integrals I are those evaluated above in Eq (E.11). The resultant E_x is then

$$E_x = \frac{2\pi a}{\lambda z} e^{-ikz} e^{-\frac{ik_\rho^2}{2z}} J_0(k_\rho a) \sin\phi \frac{J_1\left(\frac{k_\rho a}{z}\right)}{\left(\frac{k_\rho}{z}\right) - 1} \quad (\text{E.20})$$

From a similar analysis, E_y can be found and one recombines the components using the relation

$$E_\phi = -E_x \sin\phi + E_y \cos\phi \quad (\text{E.21})$$

and the resultant field in Eq (E.16) is again obtained. One should note the necessary step of casting the initial field in terms of rectangular components before the Rayleigh-Sommerfeld equation can be correctly applied. This is due to the fact that \hat{a}_x and \hat{a}_y can be factored out of integrals.

Appendix F

Development of Example 3

In this appendix, Example 3 is developed in more detail. The initial field was described by Eq (83). On S, we have from Maxwell's equations and Eq (54),

$$\bar{E}' = \frac{1}{\sqrt{2}} J_0(k_\rho \rho') \hat{a}_x + \frac{i}{\sqrt{2}} J_0(k_\rho \rho') \hat{a}_y \quad (\text{F.1})$$

$$\begin{aligned} \bar{H}' &= -\frac{1}{\omega\mu} \frac{k_z}{\sqrt{2}} J_0(k_\rho \rho') \hat{a}_x + \frac{1}{\omega\mu} \frac{k_z}{\sqrt{2}} J_0(k_\rho \rho') \hat{a}_y \\ &\quad - \frac{i}{\omega\mu} \frac{k_\rho}{\sqrt{2}} J_1(k_\rho \rho') (\cos\phi' - \sin\phi') \hat{a}_z \end{aligned} \quad (\text{F.2})$$

The components of \bar{Q} and \bar{P} follow directly:

$$Q_+^{\prime} = 0 \quad (\text{F.3})$$

$$Q_-^{\prime} = \sqrt{2} i F_- J_0(k_\rho \rho') \quad (\text{F.4})$$

$$P_+^{\prime} = 0 \quad (\text{F.5})$$

$$P_-^{\prime} = -\sqrt{2} i F_+ J_0(k_\rho \rho') \quad (\text{F.6})$$

$$Q_2^{\prime} = P_2^{\prime} = -\frac{ik_\rho}{\sqrt{2}\omega} J_1(k_\rho \rho') (\cos\phi' - \sin\phi') \quad (\text{F.7})$$

where $F_{\pm} = \frac{1}{\omega} (k \pm k_z)$. As argued in Section IV, the F_- terms are neglected in comparison to the F_+ terms. Then, substituting into the scalar integral equations, Eqs (35) through (40), with the far field approximation and letting $\theta = 0^\circ$, one finds $\bar{Q} = 0$, $P_z = P_+ = 0$ and

$$P_- = -\frac{4\sqrt{2}\pi}{\lambda z} \left(\frac{k}{\omega}\right) e^{-ikz} e^{-\frac{ik_\rho^2}{2z}} I \quad (\text{F.8})$$

where

$$I = \int_0^a J_0(k_\rho \rho') \rho' d\rho' \int_0^{2\pi} e^{i\frac{k_\rho \rho'}{z} \cos(\phi' - \phi)} d\phi' \quad (\text{F.9})$$

Using the identity shown in Eq (E.12), the integral becomes

$$I = -2\pi \int_0^a \rho' J_0(k_\rho \rho') J_0\left(\frac{k_\rho \rho'}{z}\right) d\rho' \quad (\text{F.10})$$

With the use of an aperture function like that described in Eq (D.19), this integral is a Fourier-Bessel transform (or a Hankel transform of order zero) of $J_0(k_\rho \rho')$. The integral has a closed form solution, so

$$P_- = \frac{4\sqrt{2}\pi a}{\lambda z k_\rho^2} J_1(k_\rho a) e^{-ikz} e^{-i\frac{k_\rho^2}{2z}} \left[\frac{J_0\left(\frac{k_\rho a}{z}\right)}{\left(\frac{k_\rho}{z}\right)^2 - 1} \right] \quad (\text{F.11})$$

From Eqs (41) and (42), one finds

$$E_+ = \frac{iv}{2\sqrt{z}} P_- \quad (\text{F.12})$$

so the resultant field is

$$E_3 = \frac{2\pi i a J_1(k_\rho a)}{\lambda z k_\rho} e^{-ikz} e^{-\frac{ik_\rho^2}{2z}} \left[\frac{J_0\left(\frac{k_\rho a}{z}\right)}{\left(\frac{k_\rho}{z}\right)^2 - 1} \right] \hat{a}_+ \quad (\text{F.13})$$

This is Eq (87).

To use scalar diffraction theory, one must first obtain the rectangular components of \bar{E} as in Eq (F.1), and then assume each component can be treated independently. The equation for E_x is (for $\theta = 0^\circ$)

$$E_x = -\frac{i}{\lambda z} \int_{S'} J_0(k_\rho \rho') \frac{e^{-ikr}}{R} dS' \quad (\text{F.14})$$

With the far field approximation, one has the same integral that was solved earlier in this appendix. The resultant E_x is

$$E_x = \frac{\sqrt{z} \pi k_\rho a i}{\lambda z} J_1(k_\rho a) e^{-ikz} e^{-\frac{ik_\rho^2}{2z}} \frac{J_0\left(\frac{k_\rho a}{z}\right)}{\left[\left(\frac{k_\rho}{z}\right)^2 - k_\rho^2\right]} \quad (\text{F.15})$$

A similar development for E_y leads to

$$E_y = - \frac{\sqrt{2} \pi k_\rho a}{\lambda z} J_1(k_\rho a) e^{-ikz} e^{-\frac{ik_\rho^2}{2z}} \frac{J_0\left(\frac{k_\rho a}{z}\right)}{\left[\left(\frac{k_\rho}{z}\right)^2 - k_\rho^2\right]} \quad (\text{F.16})$$

Then, using the relation $E_+ = \frac{1}{\sqrt{2}} (E_x - iE_y)$, Eq (F.13) is again obtained for the resultant field. Thus, scalar diffraction theory and the complex field vector approach yield the same result in this region.

VITA

Mark Edward Rogers was born on 16 February 1954 in Milwaukee, Wisconsin. He graduated from high school in Mequon, Wisconsin in 1972 and attended the United States Air Force Academy where he received a Bachelor of Science degree in physics and a commission as a regular officer in the USAF on 2 June 1976. His initial assignment was the Space and Missile Test Center (SAMTEC), Vandenberg AFB, California, where he served as an operations analyst for future space programs and range optical instrumentation until entering the School of Engineering, Air Force Institute of Technology in 1978.

Permanent Address: 10303 N. Greenview Dr.
Mequon, Wisconsin 53092

UNCLASSIFIED

SECURITY CLASSIFICATION OF THIS PAGE (When Data Entered)

REPORT DOCUMENTATION PAGE		READ INSTRUCTIONS BEFORE COMPLETING FORM
1. REPORT NUMBER AFIT/GEP/PH/79D-10	2. GOVT ACCESSION NO.	3. RECIPIENT'S CATALOG NUMBER
4. TITLE (and Subtitle) THE USE OF COMPLEX FIELD VECTORS IN DIFFRACTION THEORY		5. TYPE OF REPORT & PERIOD COVERED M.S. Thesis
		6. PERFORMING ORG. REPORT NUMBER
7. AUTHOR(s) MARK E. ROGERS 1st Lt USAF		8. CONTRACT OR GRANT NUMBER(s)
9. PERFORMING ORGANIZATION NAME AND ADDRESS Air Force Institute of Technology (AFIT-EN) Wright-Patterson AFB OH 45433		10. PROGRAM ELEMENT, PROJECT, TASK AREA & WORK UNIT NUMBERS
11. CONTROLLING OFFICE NAME AND ADDRESS Air Force Institute of Technology (AFIT-EN) Wright-Patterson AFB OH 45433		12. REPORT DATE DECEMBER 1979
		13. NUMBER OF PAGES 86
14. MONITORING AGENCY NAME & ADDRESS (if different from Controlling Office)		15. SECURITY CLASS. (of this report) UNCLASSIFIED
		15a. DECLASSIFICATION/DOWNGRADING SCHEDULE
16. DISTRIBUTION STATEMENT (of this Report) Approved for Public Release; Distribution Unlimited.		
17. DISTRIBUTION STATEMENT (of the abstract entered in Block 20, if different from Report)		
18. SUPPLEMENTARY NOTES Approved for Public Release; IAW AFR 190-17 JOSEPH P. HIPPS, Major, USAF Director of Public Affairs		
19. KEY WORDS (Continue on reverse side if necessary and identify by block number) Vector Diffraction Theory Linear Polarization Rayleigh-Sommerfeld Equation Scalar Diffraction Theory Azimuthal Polarization Circular Polarization Complex Field Vectors <i>6-10</i> <i>Linear Polarization</i> <i>Scalar Diffraction Theory</i> <i>Circular Polarization</i> <i>Complex Field Vectors</i> <i>E-field</i> <i>P-field</i>		
20. ABSTRACT (Continue on reverse side if necessary and identify by block number) A rigorous solution to the diffraction problem is obtained using two complex field vectors: $\vec{Q} = \mu\vec{H} + i\sqrt{\epsilon}\vec{E}$ and $\vec{D} = \mu\vec{H} - i\sqrt{\epsilon}\vec{E}$. The field equations which are uncoupled in terms of \vec{Q} and \vec{D} can be integrated directly to yield a pair of uncoupled vector integral equations involving the tangential components of \vec{Q} and \vec{D} on an arbitrary open surface. When the surface is planar, the vector equations are expressed in a more useable set of six component integral equations. The restrictions in the derivation of		

UNCLASSIFIED

SECURITY CLASSIFICATION OF THIS PAGE(When Data Entered)

E - ... (H - ...)

ITEM 20 (Cont'd):

these latter equations are that the initial \vec{E} and \vec{H} satisfy Maxwell's equations on the open surface, and that the resultant field is calculated at least several wavelengths from the initial field. The Rayleigh-Sommerfeld equation of scalar diffraction theory is obtained as a special case of the component set of equations. A discussion of the physical meaning of these component equations lends insight into the diffraction process. The complex field vector approach is seen to be a rigorous, yet simple and straightforward, method of solving the diffraction problem.



RESI
all te
CLA
bank
synt
COM
Bloc
retrie
uncla
"Ab
shou
title
Make
dates
as se
are u
order
of th
whic
of the
repor
Depa
"Re
unde
contr
Tech
office
the hi
abbre
Direc
Inser
umen
suffi
of Ex
tion
repor
it he
AD.

UNCLASSIFIED

SECURITY CLASSIFICATION OF THIS PAGE(When Data Entered)

DATE
ILME